

Gauge & Higgs Boson Particle Listings

Heavy Bosons Other than Higgs Bosons, Axions (A^0) and Other Very Light Bosons

RIZZO	00	PR D61 016007	T. G. Rizzo, J.D. Wells
ROSNER	00	PR D61 016006	J.L. Rosner
ZARNECKI	00	EPJ C17 695	A. Zarnecki
ABBIENDI	99	EPJ C6 1	G. Abbiendi et al. (OPAL Collab.)
ABBOTT	99J	PRL 83 2896	B. Abbott et al. (DO Collab.)
ABREU	99G	PL B446 62	P. Abreu et al. (DELPHI Collab.)
ACKERSTAFF	99D	EPJ C8 3	K. Ackerstaff et al. (OPAL Collab.)
ADLOFF	99	EPJ C11 447	C. Adloff et al. (HI Collab.)
Also	EPJ C14 553 (erratum)	C. Adloff et al. (HI Collab.)	
CASALBUONI	99	PL B460 135	R. Casalbuoni et al.
CZAKON	99	PL B458 355	M. Czakon, J. Gluza, M. Zralek
ERLER	99	PL B456 68	J. Erler, P. Langacker
MARCIANO	99	PR D60 093006	W. Marciano
MASIP	99	PR D60 096005	M. Masip, A. Pomarol
NATH	99	PR D60 116004	P. Nath, M. Yamaguchi
STRUMIA	99	PL B466 107	A. Strumia
ABBOTT	98E	PRL 80 2051	B. Abbott et al. (DO Collab.)
ABBOTT	98J	PRL 81 38	B. Abbott et al. (DO Collab.)
ABE	98S	PRL 81 4806	F. Abe et al. (CDF Collab.)
ABE	98V	PRL 81 5742	F. Abe et al. (CDF Collab.)
ACCIARRI	98J	PL B433 163	M. Acciari et al. (CDF Collab.)
ACKERSTAFF	98U	EPJ C2 441	K. Ackerstaff et al. (OPAL Collab.)
BARATE	98U	EPJ C4 571	R. Barate et al. (ALEPH Collab.)
BARENBOIM	98	EPJ C1 369	G. Barenboim
CHO	98	EPJ C5 155	G. Cho, K. Hagiwara, S. Matsumoto
CONRAD	98	RMP 70 1341	J.M. Conrad, M.H. Shaevitz, T. Bolton
DONCHESKI	98	PR D58 097702	M.A. Doncheski, R.W. Robinett
GROSS-PILCHER	98	hep-ex/9810015	C. Grosso-Pilcher, G. Landsberg, M. Paterno
ABE	97F	PRL 78 2906	F. Abe et al. (CDF Collab.)
ABE	97G	PR D95 R5263	F. Abe et al. (CDF Collab.)
ABE	97S	PRL 79 2192	F. Abe et al. (CDF Collab.)
ABE	97W	PRL 79 3819	F. Abe et al. (CDF Collab.)
ABE	97X	PRL 79 4327	F. Abe et al. (CDF Collab.)
ACCIARRI	97Q	PL B412 201	M. Acciari et al. (L3 Collab.)
ARIMA	97	PR D55 19	T. Arima et al. (VENUS Collab.)
BARENBOIM	97	PR D55 4213	G. Barenboim et al. (VALE, IFIC)
DEANDREA	97	PL B409 277	A. Deandrea (MARS)
DERRICK	97	ZPHY C73 613	M. Derrick et al. (ZEUS Collab.)
GROSSMAN	97	PR D55 2768	Y. Grossman, Z. Ligeti, E. Nardi
JADACH	97	PL B408 281	S. Jadach, B.F.L. Ward, Z. Was (CERN, INPC+)
STAHL	97	ZPHY C74 73	A. Stahl, H. Voss (BOHN)
ABACHI	96C	PRL 76 3271	S. Abachi et al. (DO Collab.)
ABACHI	96D	PL B395 471	S. Abachi et al. (DO Collab.)
ABREU	96T	ZPHY C72 179	P. Abreu et al. (DELPHI Collab.)
ADAM	96C	PL B380 471	W. Adam et al. (DELPHI Collab.)
AID	96B	PL B369 173	S. Aid et al. (HI Collab.)
ALLET	96	PL B383 139	M. Allet et al. (VILL, LEUV, LOUV, WIS C)
ABACHI	95E	PL B358 405	S. Abachi et al. (DO Collab.)
ABE	95M	PRL 74 2900	F. Abe et al. (CDF Collab.)
ABE	95N	PRL 74 3538	F. Abe et al. (CDF Collab.)
BALEST	95	PR D51 2053	R. Balest et al. (CLEO Collab.)
KUZNETSOV	95	PRL 75 794	I.A. Kuznetsov et al. (PNPI, KIAE, HARV+)
KUZNETSOV	95B	PAN 58 2113	A.V. Kuznetsov, N.V. Mikheev (YARO)
Also	Translated from YAF 58 2229		
MIZUKOSHI	95	NP B443 20	J.K. Mizukoshi, O.J.P. Eboli, M.C. Gonzalez-Garcia
ABREU	94O	ZPHY C64 183	P. Abreu et al. (DELPHI Collab.)
BHATTACH...	94	PL B336 100	G. Bhattacharyya, J. Ellis, K. Sridhar (CERN)
Also	PL B338 522 (erratum)	G. Bhattacharyya, J. Ellis, K. Sridhar (CERN)	
BHATTACH...	94B	PL B338 522 (erratum)	G. Bhattacharyya, J. Ellis, K. Sridhar (CERN)
DAVIDSON	94	ZPHY C61 613	S. Davidson, D. Bailey, B.A. Campbell (CPA+)
KUZNETSOV	94B	PL B329 295	A.V. Kuznetsov, N.V. Mikheev (YARO)
KUZNETSOV	94B	JETPL 60 315	I.A. Kuznetsov et al. (PNPI, KIAE, HARV+)
Also	Translated from ZETFP 60 3111		
LEURER	94	PR D50 536	M. Leurer (REHO)
LEURER	94B	PR D49 333	M. Leurer (REHO)
Also	PRL 71 1324	M. Leurer (REHO)	
MAHANTA	94	PL B337 128	U. Mahanta (MEHTA)
SEVERIJNS	94	PRL 73 611 (erratum)	N. Severijns et al. (LOUV, WIS C, LEUV+)
VILAIN	94B	PL B332 465	P. Vilain et al. (CHARM II Collab.)
ABE	93C	PL B302 119	K. Abe et al. (VENUS Collab.)
ABE	93D	PL B304 373	T. Abe et al. (TOPAZ Collab.)
ABE	93G	PRL 71 2542	F. Abe et al. (CDF Collab.)
ABREU	93J	PL B316 420	P. Abreu et al. (DELPHI Collab.)
ACTON	93E	PL B311 391	P.D. Acton et al. (OPAL Collab.)
ADRIANI	93M	PRPL 236 1	O. Adriani et al. (L3 Collab.)
ALITTI	93	NP B400 3	J. Alitti et al. (UA2 Collab.)
BHATTACH...	93	PR D47 R3693	G. Bhattacharyya et al. (CALC, JADA, ICTP+)
BUSKULIC	93F	PL B308 425	D. Buskulic et al. (ALEPH Collab.)
DERRICK	93	PL B306 173	M. Derrick et al. (ZEUS Collab.)
RIZZO	93	PR D48 4470	T.G. Rizzo (ANL)
SEVERIJNS	93	PRL 70 4047	N. Severijns et al. (LOUV, WIS C, LEUV+)
Also	PRL 73 611 (erratum)	N. Severijns et al. (LOUV, WIS C, LEUV+)	
STERNER	93	PL B303 385	K.L. Sterner et al. (AMY Collab.)
ABREU	92D	ZPHY C53 555	P. Abreu et al. (DELPHI Collab.)
ADRIANI	92F	PL B292 472	O. Adriani et al. (L3 Collab.)
DECAMP	92	PRPL 216 253	D. Decamp et al. (ALEPH Collab.)
IMAZATO	92	PRL 69 877	J. Imazato et al. (KEK, INUS, TOKY+)
MISHRA	92	PRL 68 3499	S.R. Mishra et al. (COLU, CHIC, FNAL+)
POLAK	92B	PR D46 3871	J. Polak, M. Zralek (SILES)
ACTON	91	PL B268 122	D.P. Acton et al. (OPAL Collab.)
ACTON	91B	PL B273 338	D.P. Acton et al. (OPAL Collab.)
ADEVA	91D	PL B262 155	B. Adeva et al. (L3 Collab.)
AQUINO	91	PL B261 280	M. Aquino, A. Fernandez, A. Garcia (CINV, PUEB)
COLANGELO	91	PL B253 154	P. Colangelo, G. Nardulli (BARI)
CUNYERS	91	PL B237 173	F. Cunyfers, A.F. Falk, P.H. Frampton (DURH, HARV+)
FARAGGI	91	MPL A6 61	A.E. Faraggi, D.V. Nanopoulos (STOH)
POLAK	91	NP B343 385	J. Polak, M. Zralek (SILES)
RIZZO	91	PR D44 202	T.G. Rizzo (WIS C, ISU)
WALKER	91	APJ 376 51	T.P. Walker et al. (HSCA, OSU, CHIC+)
ABE	90F	PL B246 297	K. Abe et al. (VENUS Collab.)
ABE	90H	PR D41 1722	F. Abe et al. (CDF Collab.)
AKRAWY	90J	PL B246 285	M.Z. Akrawy et al. (OPAL Collab.)
ANTREAS YAN	90C	PL B251 204	D. Antreasyan et al. (Crystal Ball Collab.)
GONZALEZ-G...	90D	PL B240 163	M.C. Gonzalez-Garcia, J.W.F. Valle (VALE)
GRIFOLS	90	NP B331 244	J.A. Griffols, E. Masso (BARC)
GRIFOLS	90D	PR D42 3293	J.A. Griffols, E. Masso, T.G. Rizzo (BARC, CERN+)
KIM	90	PL B240 243	G.H. Kim et al. (AMY Collab.)
LOPEZ	90	PL B241 392	J.L. Lopez, D.V. Nanopoulos (TAMU)
ALBAJAR	89	ZPHY C44 15	C. Albajar et al. (UA1 Collab.)
ALBRECHT	89	ZPHY C42 349	H. Albrecht et al. (ARGUS Collab.)
BARBIERI	89B	PR D39 1229	R. Barbieri, R.N. Mohapatra (PISA, UMD)
LANGACKER	89B	PR D40 1569	P. Langacker, S. Uma Sankar (PENN)
ODAKA	89	JPSJ 58 3037	S. Otake et al. (VENUS Collab.)
ROBINETT	89	PR D39 834	R.W. Robinett (PSU)
ALBAJAR	88B	PL B209 127	C. Albajar et al. (UA1 Collab.)
BAGGER	88	PR D37 1188	J. Bagger, C. Schmidt, S. King (HARV, BOST)
BALKE	88	PR D37 177	B. Balke et al. (LBL, UC, COLO, NWES+)
BERGSTROM	88	PL B212 386	L. Bergstrom (STOH)
CUNYERS	88	PRL 60 1237	F. Cunyfers, P.H. Frampton (UNCCH)
DONCHESKI	88	PL B206 137	M.A. Doncheski, H. Grotch, R. Robinett (PSU)
DONCHESKI	88B	PR D38 412	M.A. Doncheski, H. Grotch, R.W. Robinett (PSU)
ANSARI	87D	PL B195 613	R. Ansari et al. (UA2 Collab.)
BARTEL	87B	ZPHY C36 15	W. Bartel et al. (JADE Collab.)
BEHREND	86B	PL B178 452	H.J. Behrend et al. (CELLO Collab.)
DERRICK	86	PL 166B 463	M. Derrick et al. (HRS Collab.)
Also	PR D34 3286	M. Derrick et al. (HRS Collab.)	
JODIDIO	86	PR D34 1967	A. Jodidio et al. (LBL, NWES, TRIU)
Also	PR D37 237 (erratum)	A. Jodidio et al. (LBL, NWES, TRIU)	
MOHAPATRA	86	PR D34 909	R.N. Mohapatra (UMD)
ADEVA	85B	PL 152B 439	B. Adeva et al. (Mark-J Collab.)
BERGER	85B	ZPHY C27 341	C. Berger et al. (PLUTO Collab.)
STOKER	85	PRL 54 1887	D.P. Stoker et al. (LBL, NWES, TRIU)
ADEVA	84C	PRL 53 134	B. Adeva et al. (Mark-J Collab.)
BEHREND	84	PL 140B 130	H.J. Behrend et al. (CELLO Collab.)
BERGSMAS	83	PL 122B 465	F. Bergsma et al. (CHARM Collab.)
CARR	83	PRL 51 627	J. Carr et al. (LBL, NWES, TRIU)
BEALL	82	PRL 48 848	G. Beall, M. Bander, A. Soni (UCI, UCLA)
SHANKER	82	NP B204 375	O. Shanker (TRIUM)

Axions (A^0) and Other Very Light Bosons, Searches for

AXIONS AND OTHER SIMILAR PARTICLES

Revised January 2010 by C. Hagmann (LLNL), H. Murayama (UC Berkeley), G.G. Raffelt (MPI Physics), L.J. Rosenberg (U. of Washington), and K. van Bibber (LLNL).

Introduction

In this section, we list coupling-strength and mass limits for light neutral scalar or pseudoscalar bosons that couple weakly to normal matter and radiation. Such bosons may arise from a global spontaneously broken $U(1)$ symmetry, resulting in a massless Nambu-Goldstone (NG) boson. If there is a small explicit symmetry breaking, either already in the Lagrangian or due to quantum effects such as anomalies, the boson acquires a mass and is called a pseudo-NG boson. Typical examples are axions (A^0) [1,2], familons [3] and Majorons [4], associated, respectively, with a spontaneously broken Peccei-Quinn, family and lepton-number symmetry.

A common characteristic among these light bosons ϕ is that their coupling to Standard-Model particles is suppressed by the energy scale that characterizes the symmetry breaking, *i.e.*, the decay constant f . The interaction Lagrangian is

$$\mathcal{L} = f^{-1} J^\mu \partial_\mu \phi, \quad (1)$$

where J^μ is the Noether current of the spontaneously broken global symmetry. If f is very large, these new particles interact very weakly. Detecting them would provide a window to physics far beyond what can be probed at accelerators.

Axions remain of particular interest because the Peccei-Quinn (PQ) mechanism remains perhaps the most credible scheme to preserve CP in QCD. Moreover, the cold dark matter of the universe may well consist of axions and they are searched for in dedicated experiments with a realistic chance of discovery.

Originally it was assumed that the PQ scale f_A was related to the electroweak symmetry-breaking scale $v_{\text{weak}} = (\sqrt{2}G_F)^{-1/2} = 247$ GeV. However, the associated ‘‘standard’’ and ‘‘variant’’ axions were quickly excluded—we refer to the Listings for detailed limits. Here we focus on ‘‘invisible axions’’ with $f_A \gg v_{\text{weak}}$ as the main possibility.

Axions have a characteristic two-photon vertex, inherited from their mixing with π^0 and η . It allows for the main search strategy based on axion-photon conversion in external magnetic fields [5], an effect that also can be of astrophysical interest. While for axions the product ‘‘ $A\gamma\gamma$ interaction strength \times mass’’

See key on page 405

Gauge & Higgs Boson Particle Listings Axions (A^0) and Other Very Light Bosons

is essentially fixed by the corresponding π^0 properties, one may consider more general axion-like particles (ALPs) where the two parameters are independent. Several experiments have recently explored this more general parameter space.

I. THEORY

I.1 Peccei-Quinn mechanism and axions

The QCD Lagrangian includes a CP-violating term $\mathcal{L}_\Theta = \bar{\Theta} (\alpha_s/8\pi) G^{\mu\nu a} \tilde{G}_{\mu\nu}^a$, where $-\pi \leq \bar{\Theta} \leq +\pi$ is the effective Θ parameter after diagonalizing quark masses, G is the color field strength tensor, and \tilde{G} its dual. Limits on the neutron electric dipole moment [6] imply $|\bar{\Theta}| \lesssim 10^{-10}$ even though $\bar{\Theta} = \mathcal{O}(1)$ is otherwise completely satisfactory. The spontaneously broken global Peccei-Quinn symmetry $U(1)_{\text{PQ}}$ was introduced to solve this “strong CP problem” [1], an axion being the pseudo-NG boson of $U(1)_{\text{PQ}}$ [2]. This symmetry is broken due to the axion’s anomalous triangle coupling to gluons,

$$\mathcal{L} = \left(\bar{\Theta} - \frac{\phi_A}{f_A} \right) \frac{\alpha_s}{8\pi} G^{\mu\nu a} \tilde{G}_{\mu\nu}^a, \quad (2)$$

where ϕ_A is the axion field and f_A the axion decay constant. Color anomaly factors have been absorbed in the normalization of f_A which is defined by this Lagrangian. Thus normalized, f_A is the quantity that enters all low-energy phenomena [7]. Non-perturbative effects induce a potential for ϕ_A whose minimum is at $\phi_A = \bar{\Theta} f_A$, thereby canceling the $\bar{\Theta}$ term in the QCD Lagrangian and thus restoring CP symmetry.

The resulting axion mass is given by $m_A f_A \approx m_\pi f_\pi$ where $m_\pi = 135$ MeV and $f_\pi \approx 92$ MeV. In more detail one finds

$$m_A = \frac{z^{1/2}}{1+z} \frac{f_\pi m_\pi}{f_A} = \frac{0.60 \text{ meV}}{f_A/10^{10} \text{ GeV}}, \quad (3)$$

where $z = m_u/m_d$. We have used the canonical value $z = 0.56$ [8], although the range $z = 0.35\text{--}0.60$ is plausible [9].

Originally one assumed $f_A \sim v_{\text{weak}}$ [1,2]. Tree-level flavor conservation fixes the axion properties in terms of a single parameter $\tan\beta$, the ratio of the vacuum expectation values of two Higgs fields that appear as a minimal ingredient. This “standard axion” is excluded after extensive searches [10]. A narrow peak structure observed in positron spectra from heavy ion collisions [11] suggested an axion-like particle of mass 1.8 MeV that decays into e^+e^- , but extensive follow-up searches were negative. “Variant axion models” were proposed which keep $f_A \sim v_{\text{weak}}$ while dropping the constraint of tree-level flavor conservation [12], but these models are also excluded [13].

Axions with $f_A \gg v_{\text{weak}}$ evade all current experimental limits. One generic class of models invokes “hadronic axions” where new heavy quarks carry $U(1)_{\text{PQ}}$ charges, leaving ordinary quarks and leptons without tree-level axion couplings. The prototype is the KSVZ model [14], where in addition the heavy quarks are electrically neutral. Another generic class requires at least two Higgs doublets and ordinary quarks and leptons carry PQ charges, the prototype being the DFSZ model [15]. All of these models contain at least one electroweak singlet

scalar that acquires a vacuum expectation value and thereby breaks the PQ symmetry. The KSVZ and DFSZ models are frequently used as generic examples, but other models exist where both heavy quarks and Higgs doublets carry PQ charges.

I.2 Model-dependent axion couplings

Although the generic axion interactions scale approximately with f_π/f_A from the corresponding π^0 couplings, there are non-negligible model-dependent factors and uncertainties. The axion’s two-photon interaction plays a key role for many searches,

$$\mathcal{L}_{A\gamma\gamma} = \frac{G_{A\gamma\gamma}}{4} F_{\mu\nu} \tilde{F}^{\mu\nu} \phi_A = -G_{A\gamma\gamma} \mathbf{E} \cdot \mathbf{B} \phi_A, \quad (4)$$

where F is the electromagnetic field-strength tensor and \tilde{F} its dual. The coupling constant is

$$\begin{aligned} G_{A\gamma\gamma} &= \frac{\alpha}{2\pi f_A} \left(\frac{E}{N} - \frac{2}{3} \frac{4+z}{1+z} \right) \\ &= \frac{\alpha}{2\pi} \left(\frac{E}{N} - \frac{2}{3} \frac{4+z}{1+z} \right) \frac{1+z}{z^{1/2}} \frac{m_A}{m_\pi f_\pi}, \end{aligned} \quad (5)$$

where E and N are the electromagnetic and color anomalies of the axial current associated with the axion. In grand unified models, and notably for DFSZ [15], $E/N = 8/3$, whereas for KSVZ [14] $E/N = 0$ if the electric charge of the new heavy quark is taken to vanish. In general, a broad range of E/N values is possible [16]. The two-photon decay width is

$$\Gamma_{A \rightarrow \gamma\gamma} = \frac{G_{A\gamma\gamma}^2 m_A^3}{64\pi} = 1.1 \times 10^{-24} \text{ s}^{-1} \left(\frac{m_A}{\text{eV}} \right)^5. \quad (6)$$

The second expression uses Eq. (5) with $z = 0.56$ and $E/N = 0$. Axions decay faster than the age of the universe if $m_A \gtrsim 20$ eV.

The interaction with fermions f has derivative form and is invariant under a shift $\phi_A \rightarrow \phi_A + \phi_0$ as behoves a NG boson,

$$\mathcal{L}_{Aff} = \frac{C_f}{2f_A} \bar{\Psi}_f \gamma^\mu \gamma_5 \Psi_f \partial_\mu \phi_A. \quad (7)$$

Here, Ψ_f is the fermion field, m_f its mass, and C_f a model-dependent coefficient. The dimensionless combination $g_{Aff} \equiv C_f m_f / f_A$ plays the role of a Yukawa coupling and $\alpha_{Aff} \equiv g_{Aff}^2 / 4\pi$ of a “fine-structure constant.” The often-used pseudoscalar form $\mathcal{L}_{Aff} = -i(C_f m_f / f_A) \bar{\Psi}_f \gamma_5 \Psi_f \phi_A$ need not be equivalent to the appropriate derivative structure, for example when two NG bosons are attached to one fermion line as in axion emission by nucleon bremsstrahlung [17].

In the DFSZ model [15], the tree-level coupling coefficient to electrons is

$$C_e = \frac{\cos^2 \beta}{3}, \quad (8)$$

where $\tan\beta$ is the ratio of two Higgs vacuum expectation values that are generic to this and similar models.

For nucleons, $C_{n,p}$ are related to axial-vector current matrix elements by generalized Goldberger-Treiman relations,

$$\begin{aligned} C_p &= (C_u - \eta) \Delta u + (C_d - \eta z) \Delta d + (C_s - \eta w) \Delta s, \\ C_n &= (C_u - \eta) \Delta d + (C_d - \eta z) \Delta u + (C_s - \eta w) \Delta s. \end{aligned} \quad (9)$$

Gauge & Higgs Boson Particle Listings

Axions (A^0) and Other Very Light Bosons

Here, $\eta = (1 + z + w)^{-1}$ with $z = m_u/m_d$ and $w = m_u/m_s \ll z$ and the Δq are given by the axial vector current matrix element $\Delta q S_\mu = \langle p | \bar{q} \gamma_\mu \gamma_5 q | p \rangle$ with S_μ the proton spin.

Neutron beta decay and strong isospin symmetry considerations imply $\Delta u - \Delta d = F + D = 1.269 \pm 0.003$, whereas hyperon decays and flavor SU(3) symmetry imply $\Delta u + \Delta d - 2\Delta s = 3F - D = 0.586 \pm 0.031$ [19]. The strange-quark contribution is $\Delta s = -0.08 \pm 0.01_{\text{stat}} \pm 0.05_{\text{sys}}$ from the COMPASS experiment [18], and $\Delta s = -0.085 \pm 0.008_{\text{exp}} \pm 0.013_{\text{theor}} \pm 0.009_{\text{evol}}$ from HERMES [19], in agreement with each other and with an early estimate of $\Delta s = -0.11 \pm 0.03$ [20]. We thus adopt $\Delta u = 0.84 \pm 0.02$, $\Delta d = -0.43 \pm 0.02$ and $\Delta s = -0.09 \pm 0.02$, very similar to what was used in the axion literature.

The uncertainty of the axion-nucleon couplings is dominated by the uncertainty $z = m_u/m_d = 0.35\text{--}0.60$ that we mentioned earlier. For hadronic axions $C_{u,d,s} = 0$ so that $-0.51 < C_p < -0.36$ and $0.10 > C_n > -0.05$. Therefore it is well possible that $C_n = 0$ whereas C_p does not vanish within the plausible z range. In the DFSZ model, $C_u = \frac{1}{3} \sin^2 \beta$ and $C_d = \frac{1}{3} \cos^2 \beta$ and C_n and C_p as functions of β and z do not vanish simultaneously.

The axion-pion interaction is given by the Lagrangian [21]

$$\mathcal{L}_{A\pi} = \frac{C_{A\pi}}{f_\pi f_A} (\pi^0 \pi^+ \partial_\mu \pi^- + \pi^0 \pi^- \partial_\mu \pi^+ - 2\pi^+ \pi^- \partial_\mu \pi^0) \partial_\mu \phi_A, \quad (10)$$

where $C_{A\pi} = (1 - z)/[3(1 + z)]$ in hadronic models. The chiral symmetry-breaking Lagrangian provides an additional term $\mathcal{L}'_{A\pi} \propto (m_\pi^2/f_\pi f_A) (\pi^0 \pi^0 + 2\pi^- \pi^+) \pi^0 \phi_A$. For hadronic axions it vanishes identically, in contrast to the DFSZ model (Roberto Peccei, private communication).

II. LABORATORY SEARCHES

II.1 Photon regeneration

Searching for “invisible axions” is extremely challenging. The most promising approaches rely on the axion-two-photon vertex, allowing for axion-photon conversion in external electric or magnetic fields [5]. For the Coulomb field of a charged particle, the conversion is best viewed as a scattering process, $\gamma + Ze \leftrightarrow Ze + A$, called Primakoff effect [22]. In the other extreme of a macroscopic field, usually a large-scale B -field, the momentum transfer is small, the interaction coherent over a large distance, and the conversion is best viewed as an axion-photon oscillation phenomenon in analogy to neutrino flavor oscillations [23].

Photons propagating through a transverse magnetic field, with incident \mathbf{E}_γ and magnet \mathbf{B} parallel, may convert into axions. For $m_A^2 L/2\omega \ll 2\pi$, where L is the length of the B field region and ω the photon energy, the resultant axion beam is coherent with the incident photon beam and the conversion probability is $\Pi \sim (1/4)(G_{A\gamma\gamma} BL)^2$. A practical realization uses a laser beam propagating down the bore of a superconducting dipole magnet (like the bending magnets in high-energy accelerators). If another magnet is in line with the first, but shielded by an optical barrier, then photons may

be regenerated from the pure axion beam [24]. The overall probability $P(\gamma \rightarrow A \rightarrow \gamma) = \Pi^2$.

The first such experiment utilized two magnets of length $L = 4.4$ m and $B = 3.7$ T and found $G_{A\gamma\gamma} < 6.7 \times 10^{-7}$ GeV $^{-1}$ at 95% CL for $m_A < 1$ meV [25]. More recently, several such experiments were performed (see Listings), improving the limit to $G_{A\gamma\gamma} < 3.5 \times 10^{-7}$ GeV $^{-1}$ at 3σ in the massless limit [26]. Some of these experiments have also reported limits for scalar bosons where the photon \mathbf{E}_γ must be chosen perpendicular to the magnet \mathbf{B} .

A new concept, resonantly-enhanced photon regeneration, may open unexplored regions of coupling strength [27]. In this scheme, both the production and detection magnets are within Fabry-Perot optical cavities and actively locked in frequency. The $\gamma \rightarrow A \rightarrow \gamma$ rate is enhanced by a factor $2\mathcal{F}\mathcal{F}'/\pi^2$ relative to a single-pass experiment, where \mathcal{F} and \mathcal{F}' are the finesses of the two cavities. The resonant enhancement could be of order $10^{(10-12)}$, improving the $G_{A\gamma\gamma}$ sensitivity by $10^{(2.5-3)}$. Another new concept involves axion absorption and emission between electromagnetic fields within a high finesse optical cavity [28]. A signal appears as resonant sidebands on the carrier. This technique could be sensitive in the mass range $10^{-6}\text{--}10^{-4}$ eV and reach the KSVZ line after one year of operation.

II.2 Photon polarization

An alternative to regenerating the lost photons is to use the beam itself to detect conversion: the polarization of light propagating through a transverse B field suffers dichroism and birefringence [29]. Dichroism: The E_\parallel component, but not E_\perp , is depleted by axion production, causing a small rotation of linearly polarized light. For $m_A^2 L/2\omega \ll 2\pi$ the effect is independent of m_A , for heavier axions it oscillates and diminishes as m_A increases, and it vanishes for $m_A > \omega$. Birefringence: This rotation occurs because there is mixing of virtual axions in the E_\parallel state, but not for E_\perp . Hence, linearly polarized light will develop elliptical polarization. Higher-order QED also induces vacuum birefringence. A search for these effects was performed on the same dipole magnets in the early experiment above [30]. The dichroic rotation gave a stronger limit than the ellipticity rotation: $G_{A\gamma\gamma} < 3.6 \times 10^{-7}$ GeV $^{-1}$ at 95% CL for $m_A < 5 \times 10^{-4}$ eV. The ellipticity limits are better at higher masses, as they fall off smoothly and do not terminate at m_A .

In 2006 the PVLAS collaboration reported a signature of magnetically induced vacuum dichroism that could be interpreted as the effect of a pseudoscalar with $m_A = 1\text{--}1.5$ meV and $G_{A\gamma\gamma} = (1.6\text{--}5) \times 10^{-6}$ GeV $^{-1}$ [31]. Since then, these findings are attributed to instrumental artifacts [32]. This particle interpretation is also excluded by the above photon regeneration searches that were triggered by the original PVLAS result.

II.3 Long-range forces

New bosons would mediate long-range forces, which are severely constrained by “fifth force” experiments [33]. Those

See key on page 405

Gauge & Higgs Boson Particle Listings Axions (A^0) and Other Very Light Bosons

looking for new mass-spin couplings provide significant constraints on pseudoscalar bosons [34]. However, they do not yet cover realistic parameters for invisible axion models because they are only sensitive for small m_A . The corresponding coupling strengths scale with $f_A^{-1} \approx m_A/m_\pi f_\pi$ and are too small to be detected. Still, these efforts provide constraints on more general low-mass bosons.

III. AXIONS FROM ASTROPHYSICAL SOURCES

III.1 Stellar energy-loss limits:

Low-mass weakly-interacting particles (neutrinos, gravitons, axions, baryonic or leptonic gauge bosons, *etc.*) are produced in hot astrophysical plasmas, and can thus transport energy out of stars. The coupling strength of these particles with normal matter and radiation is bounded by the constraint that stellar lifetimes or energy-loss rates not conflict with observation [35–37].

We begin this discussion with our Sun and concentrate on hadronic axions. They are produced predominantly by the Primakoff process $\gamma + Ze \rightarrow Ze + A$. Integrating over a standard solar model yields the axion luminosity [49]

$$L_A = G_{10}^2 1.85 \times 10^{-3} L_\odot, \quad (11)$$

where $G_{10} = G_{A\gamma\gamma} \times 10^{10}$ GeV. The maximum of the spectrum is at 3.0 keV, the average at 4.2 keV, and the number flux at Earth is $G_{10}^2 3.75 \times 10^{11}$ cm⁻² s⁻¹. The solar photon luminosity is fixed, so axion losses require enhanced nuclear energy production and thus enhanced neutrino fluxes. The all-flavor measurements by SNO together with a standard solar model imply $L_A \lesssim 0.10 L_\odot$, corresponding to $G_{10} \lesssim 7$ [38], mildly superseding a similar limit from helioseismology [39].

A more restrictive limit derives from globular-cluster (GC) stars that allow for detailed tests of stellar-evolution theory. The stars on the horizontal branch (HB) in the color-magnitude diagram have reached helium burning with a core-averaged energy release of about 80 erg g⁻¹ s⁻¹, compared to Primakoff axion losses of $G_{10}^2 30$ erg g⁻¹ s⁻¹. The accelerated consumption of helium reduces the HB lifetime by about 80/(80+30 G_{10}^2). Number counts of HB stars in 15 GCs compared with the number of red giants (that are not much affected by Primakoff losses) reveal agreement with expectations within 20–40% in any one GC and overall on the 10% level [36]. Therefore, a reasonably conservative limit is

$$G_{A\gamma\gamma} \lesssim 1 \times 10^{-10} \text{ GeV}^{-1}, \quad (12)$$

although a detailed error budget is not available.

We translate this constraint on $G_{A\gamma\gamma}$ to $f_A > 2.3 \times 10^7$ GeV ($m_A < 0.3$ eV), using $z = 0.56$ and $E/N = 0$ as in the KSVZ model, and show the excluded range in Figure 1. For the DFSZ model with $E/N = 8/3$, the corresponding limits are slightly less restrictive, $f_A > 0.8 \times 10^7$ GeV ($m_A < 0.7$ eV). The exact high-mass end of the exclusion range has not been determined. The relevant temperature is around 10 keV and the average photon energy is therefore around 30 keV. The excluded m_A range thus certainly extends beyond the shown 100 keV.

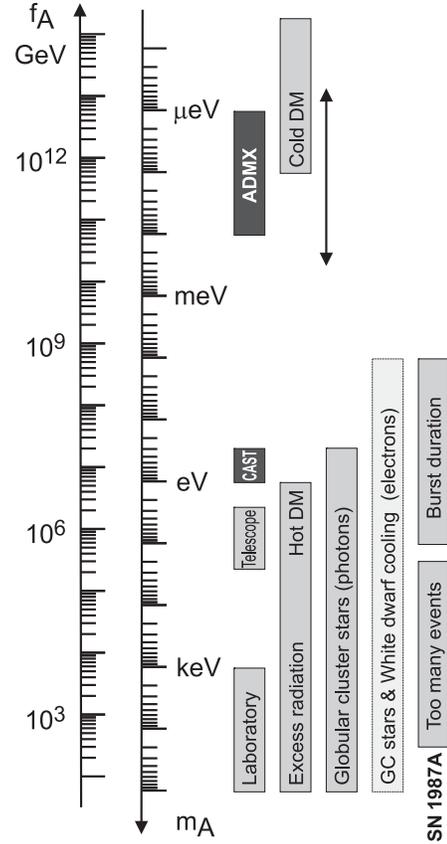


Figure 1: Exclusion ranges as described in the text. The dark intervals are the approximate CAST and ADMX search ranges. Limits on coupling strengths are translated into limits on m_A and f_A using $z = 0.56$ and the KSVZ values for the coupling strengths. The “Laboratory” bar is a rough representation of the exclusion range for standard or variant axions. The “GC stars and white-dwarf cooling” range uses the DFSZ model with an axion-electron coupling corresponding to $\cos^2 \beta = 1/2$. The Cold Dark Matter exclusion range is particularly uncertain. We show the benchmark case from the misalignment mechanism.

If axions couple directly to electrons, the dominant emission processes are $\gamma + e^- \rightarrow e^- + A$ and $e^- + Ze \rightarrow Ze + e^- + A$. Moreover, bremsstrahlung is efficient in white dwarfs (WDs), where the Primakoff and Compton processes are suppressed by the large plasma frequency. The enhanced energy losses would delay helium ignition in GC stars, implying $\alpha_{Aee} \lesssim 0.5 \times 10^{-26}$ [40]. Enhanced WD cooling leads to a similar limit from the WD luminosity function [41]. For pulsationally unstable WDs (ZZ Ceti stars), the period decrease \dot{P}/P is a measure of the cooling speed. A well-studied case is the star G117–B15A, where the measured \dot{P}/P implies [42]

$$\alpha_{Aee} < 1.3 \times 10^{-27} \quad (13)$$

Gauge & Higgs Boson Particle Listings

Axions (A^0) and Other Very Light Bosons

at a statistical 95% CL. (We have corrected the published limit for an apparent misprint.) This result is equivalent to $g_{Aee} < 1.3 \times 10^{-13}$ or in the DFSZ model to $f_A > 1.3 \times 10^9 \text{ GeV} \cos^2 \beta$ and $m_A < 4.5 \text{ meV}/\cos^2 \beta$. We show these constraints in Figure 1 for $\cos^2 \beta = 1/2$.

Similar constraints derive from the measured duration of the neutrino signal of the supernova SN 1987A. Numerical simulations for a variety of cases, including axions and Kaluza-Klein gravitons, reveal that the energy-loss rate of a nuclear medium at the density $3 \times 10^{14} \text{ g cm}^{-3}$ and temperature 30 MeV should not exceed about $1 \times 10^{19} \text{ erg g}^{-1} \text{ s}^{-1}$ [36]. The energy-loss rate from nucleon bremsstrahlung, $N + N \rightarrow N + N + A$, is $(C_N/2f_A)^2 (T^4/\pi^2 m_N) F$. Here F is a numerical factor that represents an integral over the dynamical spin-density structure function because axions couple to the nucleon spin. For realistic conditions, even after considerable effort, one is limited to a heuristic estimate leading to $F \approx 1$ [37].

The SN 1987A limits are of particular interest for hadronic axions where the bounds on α_{Aee} are moot. Within uncertainties of $z = m_u/m_d$ a reasonable choice for the coupling constants is then $C_p = -0.4$ and $C_n = 0$. Using a proton fraction of 0.3, $F = 1$, and $T = 30 \text{ MeV}$ one finds [37]

$$f_A \gtrsim 4 \times 10^8 \text{ GeV} \quad \text{and} \quad m_A \lesssim 16 \text{ meV}. \quad (14)$$

If axions interact sufficiently strongly they are trapped. Only about three orders of magnitude in g_{ANN} or m_A are excluded, a range shown somewhat schematically in Figure 1. For even larger couplings, the axion flux would have been negligible, yet it would have triggered additional events in the detectors, excluding a further range [43]. A possible gap between these two SN 1987A arguments was discussed as the ‘‘hadronic axion window’’ under the assumption that $G_{A\gamma\gamma}$ was anomalously small [44]. This range is now excluded by hot dark matter bounds (see below).

III.2 Searches for solar axions

Instead of using stellar energy losses to derive axion limits, one can also search directly for these fluxes, notably from the Sun. The main focus has been on axion-like particles with a two-photon vertex. They are produced by the Primakoff process with a flux given by Equation 11 and can be detected at Earth with the reverse process in a macroscopic B -field (‘‘axion helioscope’’) [5]. The average energy of solar axions of 4.2 keV implies a photon-axion oscillation length in vacuum of $2\pi(2\omega/m_A^2) \sim \mathcal{O}(1 \text{ mm})$, precluding the vacuum mixing from achieving its theoretical maximum in any practical magnet. However, one can endow the photon with an effective mass in a gas, $m_\gamma = \omega_{\text{plas}}$, thus matching the axion and photon dispersion relations [45].

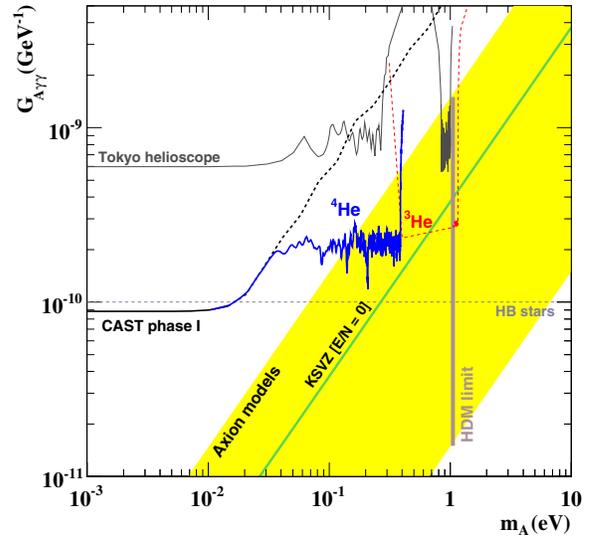


Figure 2: Solar exclusion plot for axion-like particles [50]. The red dashed line is the sensitivity of the ongoing ^3He phase of CAST. The vertical line (HDM) is the hot dark-matter limit [59]. The yellow band represents models with $0.07 < |E/N - 1.92| < 0.7$, the green solid line corresponds to KSVZ axions.

An early implementation of these ideas used a conventional dipole magnet, with a conversion volume of variable-pressure gas with a xenon proportional chamber as x-ray detector [46]. The conversion magnet was fixed in orientation and collected data for about 1000 s/day. Axions were excluded for $G_{A\gamma\gamma} < 3.6 \times 10^{-9} \text{ GeV}^{-1}$ for $m_A < 0.03 \text{ eV}$, and $G_{A\gamma\gamma} < 7.7 \times 10^{-9} \text{ GeV}^{-1}$ for $0.03 < m_A < 0.11 \text{ eV}$ at 95% CL.

Later, the Tokyo axion helioscope used a superconducting magnet on a tracking mount, viewing the Sun continuously. They reported $G_{A\gamma\gamma} < 6 \times 10^{-10} \text{ GeV}^{-1}$ for $m_A < 0.3 \text{ eV}$ [47]. Recently this experiment was recommissioned and a similar limit for masses around 1 eV was reported [48]. These exclusion ranges are shown in Figure 2.

The most recent helioscope CAST (CERN Axion Solar Telescope) uses a decommissioned LHC dipole magnet on a tracking mount. The hardware includes grazing-incidence x-ray optics with solid-state x-ray detectors, as well as a novel x-ray Micromegas position-sensitive gaseous detector. CAST has established a 95% CL limit $G_{A\gamma\gamma} < 8.8 \times 10^{-11} \text{ GeV}^{-1}$ for $m_A < 0.02 \text{ eV}$ [49]. To cover larger masses and to ‘‘cross the axion line,’’ the magnet bores are filled with a gas at varying pressure. The runs with ^4He cover masses up to about 0.4 eV [50], providing the limits shown in Figure 2. Ongoing runs with ^3He gas have explored masses up to 0.85 eV, aiming to about 1.16 eV, but final results are not yet available.

Other Primakoff searches for solar axions have been carried out using crystal detectors, exploiting the coherent conversion of axions into photons when the axion angle of incidence satisfies

See key on page 405

Gauge & Higgs Boson Particle Listings Axions (A^0) and Other Very Light Bosons

a Bragg condition with a crystal plane [51]. However, none of these limits is more restrictive than the one derived from solar neutrinos that was discussed earlier.

Another idea is to look at the Sun with an x-ray satellite when the Earth is in between. Solar axions would convert in the Earth magnetic field on the far side and could be detected [52]. The sensitivity to $G_{A\gamma\gamma}$ could be comparable to CAST, but only for much smaller m_A .

III.3 Conversion of astrophysical photon fluxes

Large-scale B fields exist in astrophysics that can induce axion-photon oscillations. In practical cases, B is much smaller than in the laboratory, whereas the conversion region L is much larger. Therefore, while the product BL can be large, realistic sensitivities are usually restricted to very low-mass particles, far away from the “axion line” in a plot like Figure 2.

One example is SN 1987A, which would have emitted a burst of axion-like particles due to the Primakoff production in its core. They would have partially converted into γ -rays in the galactic B -field. The absence of a γ -ray burst in coincidence with SN 1987A neutrinos provides a limit $G_{A\gamma\gamma} \lesssim 1 \times 10^{-11} \text{ GeV}^{-1}$ for $m_A \lesssim 10^{-9} \text{ eV}$ [53], the most restrictive limit for very small m_A . Axion-like particles from other stars can be converted to photons, but no tangible new limits or signatures seem to have appeared.

Conversely, photons from distant sources could transform to axion-like particles, depleting the original flux. This mechanism was proposed as an alternative to cosmic acceleration for explaining the apparent dimming of distant SNe Ia [54]. However, this effect would apply to all distant sources, including quasars and the cosmic microwave background and would depend on energy. All things considered, this mechanism can only play a subdominant role [55]. On the other hand, very recently the observed scatter of x/ γ -ray fluxes from active galactic nuclei was interpreted in terms of very low-mass ALPs [56].

High-energy γ -rays are typically produced in magnetized environments where cosmic rays are accelerated. The conversion into axion-like particles can then, in principle, imprint observable features on the spectrum for a range of coupling constants not excluded by other arguments [57].

IV. COSMIC AXIONS

IV.1 Cosmic axion populations

In the early universe, axions are produced by processes involving quarks and gluons [58]. After color confinement, the dominant thermalization process is $\pi + \pi \leftrightarrow \pi + A$ [21]. The resulting axion population would contribute a hot dark matter component in analogy to massive neutrinos. Cosmological precision data provide restrictive constraints on a possible hot dark-matter fraction that translate into $m_A < 0.4\text{--}1.0 \text{ eV}$ at the 95% statistical CL [59]. The spread of published limits reflects the use of different cosmological data sets.

For $m_A \gtrsim 20 \text{ eV}$, axions decay fast on a cosmic time scale, removing the axion population while injecting photons. This

excess radiation provides additional limits up to very large axion masses [60]. An anomalously small $G_{A\gamma\gamma}$ provides no loophole because suppressing decays leads to thermal axions overdominating the mass density of the universe.

The main cosmological interest in axions derives from their possible role as cold dark matter (CDM). In addition to thermal processes, axions are abundantly produced by the “misalignment mechanism” [61]. After the breakdown of the PQ symmetry, the axion field relaxes somewhere in the “bottom of the wine bottle” potential. Near the QCD epoch, instanton effects explicitly break the PQ symmetry, the very effect that causes dynamical PQ symmetry restoration. This “tilting of the wine bottle” drives the axion field toward the CP-conserving minimum, thereby exciting coherent oscillations of the axion field that ultimately represent a condensate of CDM. The cosmic mass density in this homogeneous field mode is [62]

$$\Omega_A h^2 \approx 0.7 \left(\frac{f_A}{10^{12} \text{ GeV}} \right)^{7/6} \left(\frac{\bar{\Theta}_i}{\pi} \right)^2, \quad (15)$$

where h is the present-day Hubble expansion parameter in units of $100 \text{ km s}^{-1} \text{ Mpc}^{-1}$, and $-\pi \leq \bar{\Theta}_i \leq \pi$ is the initial “misalignment angle” relative to the CP-conserving position. If the PQ symmetry breakdown takes place after inflation, $\bar{\Theta}_i$ will take on different values in different patches of the universe. The average contribution is [62]

$$\Omega_A h^2 \approx 0.3 \left(\frac{f_A}{10^{12} \text{ GeV}} \right)^{7/6}. \quad (16)$$

Comparing with the measured CDM density of $\Omega_{\text{CDM}} h^2 \approx 0.13$ implies that axions with $m_A \approx 10 \text{ } \mu\text{eV}$ provide the dark matter, whereas smaller masses are excluded (Figure 1).

This density sets only a rough scale for the expected m_A . The mass of CDM axions could be significantly smaller or larger than $10 \text{ } \mu\text{eV}$. Apart from the overall particle physics uncertainties, the cosmological sequence of events is crucial. Assuming axions make up CDM, much smaller masses are possible if inflation took place after the PQ transition and the initial value $\bar{\Theta}_i$ was small (“anthropic axion window” [63]). Conversely, if the PQ transition took place after inflation, there are additional sources for nonthermal axions, notably the decay of cosmic strings and domain walls, although these populations are comparable to the misalignment contribution [62].

If the reheat temperature after inflation is too small to restore PQ symmetry, the axion field is present during inflation. It is subject to quantum fluctuations, leading to isocurvature fluctuations that are severely constrained [64].

In the opposite case without inflation after the PQ transition, the spatial axion density variations are large at the QCD transition and they are not erased by free streaming. When matter begins to dominate the universe, gravitationally bound “axion mini clusters” form promptly [65]. A significant fraction of CDM axions can reside in these bound objects.

Gauge & Higgs Boson Particle Listings

Axions (A^0) and Other Very Light Bosons

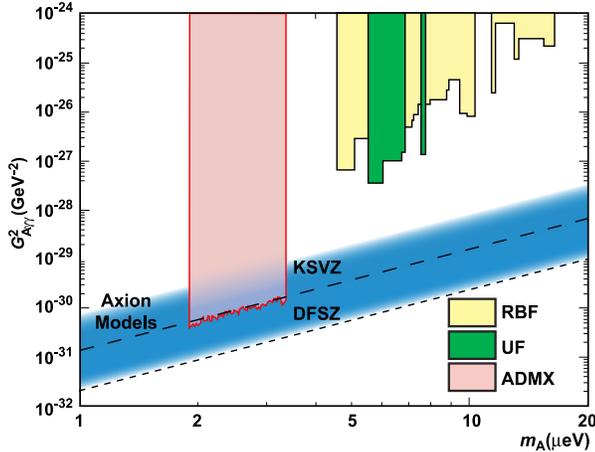


Figure 3: Exclusion region reported from the microwave cavity experiments RBF and UF [71] and ADMX [72]. A local dark-matter density of 450 MeV cm^{-3} is assumed.

IV.2 Telescope searches

The two-photon decay is extremely slow for axions with masses in the CDM regime, but could be detectable for eV masses. The signature would be a quasi-monochromatic emission line from galaxies and galaxy clusters. The expected optical line intensity for DFSZ axions is similar to the continuum night emission. An early search in three rich Abell clusters [66], and a recent search in two rich Abell clusters [67], exclude the “Telescope” range in Figure 1 unless the axion-photon coupling is strongly suppressed. Of course, axions in this mass range would anyway provide an excessive hot DM contribution.

Very-mass axions in halos produce a weak quasi-monochromatic radio line. Virial velocities in undisrupted dwarf galaxies are very low, and the axion decay line would therefore be extremely narrow. A search with the Haystack radio telescope on three nearby dwarf galaxies provided a limit $G_{A\gamma\gamma} < 1.0 \times 10^{-9} \text{ GeV}^{-1}$ at 96% CL for $298 < m_A < 363 \text{ } \mu\text{eV}$ [68]. However, this combination of m_A and $G_{A\gamma\gamma}$ does not exclude plausible axion models.

IV.3 Microwave cavity experiments

The limits of Figure 1 suggest that axions, if they exist, provide a significant fraction or even perhaps all of the cosmic CDM. In a broad range of the plausible m_A range for CDM, galactic halo axions may be detected by their resonant conversion into a quasi-monochromatic microwave signal in a high-Q electromagnetic cavity permeated by a strong static B field [5,69]. The cavity frequency is tunable, and the signal is maximized when the frequency is the total axion energy, rest mass plus kinetic energy, of $\nu = (m_A/2\pi) [1 + \mathcal{O}(10^{-6})]$, the width above the rest mass representing the virial distribution in the galaxy. The frequency spectrum may also contain finer structure from axions more recently fallen into the galactic potential and not yet completely virialized [70].

The feasibility of this technique was established in early experiments of relatively small sensitive volume, $\mathcal{O}(1 \text{ liter})$, with HFET-based amplifiers, setting limits in the range $4.5 < m_A < 16.3 \text{ } \mu\text{eV}$ [71], but lacking by 2–3 orders of magnitude the sensitivity required to detect realistic axions. Later, ADMX ($B \sim 8 \text{ T}$, $V \sim 200 \text{ liters}$) has achieved sensitivity to KSVZ axions, assuming they saturate the local dark matter density and are well virialized, over the mass range $1.9\text{--}3.3 \text{ } \mu\text{eV}$ [72]. Should halo axions have a component not yet virialized, ADMX is sensitive to DFSZ axions [73]. The corresponding 90% CL exclusion regions shown in Figure 3 are normalized to an assumed local CDM density of $7.5 \times 10^{-25} \text{ g cm}^{-3}$ (450 MeV cm^{-3}). Very recently the ADMX experiment has commissioned an upgrade [74] that replaces the microwave HFET amplifiers by near quantum-limited low-noise dc SQUID microwave amplifiers [75], allowing for a significantly improved sensitivity. Alternatively, a Rydberg atom single-photon detector [76] can in principle evade the standard quantum limit for coherent photon detection. Efforts are underway to incorporate Rydberg atom systems in RF cavity axion searches [77].

Conclusions

Experimental, astrophysical, and cosmological limits have been refined and indicate that axions, if they exist, very likely have very low mass, $m_A \lesssim 10 \text{ meV}$, suggesting that axions are a non-negligible fraction of the cosmic CDM. The upgraded versions of the ADMX experiment will ultimately cover the range $1\text{--}100 \text{ } \mu\text{eV}$ with a sensitivity allowing one to detect such axions, unless the local DM density is unexpectedly small or the axion-photon coupling anomalously weak. Other experimental techniques remain of interest to search for axion-like particles, although at present no method besides the DM search is known that could detect realistic axions obeying the astrophysical and cosmological limits, and fulfilling the QCD-implied relationship between mass and coupling strength.

References

1. R.D. Peccei and H. Quinn, Phys. Rev. Lett. **38**, 1440 (1977), Phys. Rev. **D16**, 1791 (1977).
2. S. Weinberg, Phys. Rev. Lett. **40**, 223 (1978); F. Wilczek, Phys. Rev. Lett. **40**, 279 (1978).
3. F. Wilczek, Phys. Rev. Lett. **49**, 1549 (1982).
4. Y. Chikashige, R.N. Mohapatra, and R.D. Peccei, Phys. Lett. **98B**, 265 (1981); G.B. Gelmini and M. Roncadelli, Phys. Lett. **99B**, 411 (1981).
5. P. Sikivie, Phys. Rev. Lett. **51**, 1415 (1983) and Erratum *ibid.*, **52**, 695 (1984).
6. C.A. Baker *et al.*, Phys. Rev. Lett. **97**, 131801 (2006).
7. H. Georgi, D.B. Kaplan, and L. Randall, Phys. Lett. **B169**, 73 (1986).
8. H. Leutwyler, Phys. Lett. **B378**, 313 (1996).
9. Mini review on Quark Masses in: C. Amsler *et al.* (Particle Data Group), Phys. Lett. **B667**, 1 (2008).
10. T.W. Donnelly *et al.*, Phys. Rev. **D18**, 1607 (1978); S. Barshay *et al.*, Phys. Rev. Lett. **46**, 1361 (1981);

See key on page 405

Gauge & Higgs Boson Particle Listings Axions (A^0) and Other Very Light Bosons

- A. Barroso and N.C. Mukhopadhyay, Phys. Lett. **B106**, 91 (1981);
R.D. Peccei, in *Proceedings of Neutrino '81*, Honolulu, Hawaii, Vol. 1, p. 149 (1981);
L.M. Krauss and F. Wilczek, Phys. Lett. **B173**, 189 (1986).
11. J. Schweppe *et al.*, Phys. Rev. Lett. **51**, 2261 (1983);
T. Cowan *et al.*, Phys. Rev. Lett. **54**, 1761 (1985).
 12. R.D. Peccei, T.T. Wu, and T. Yanagida, Phys. Lett. **B172**, 435 (1986).
 13. W.A. Bardeen, R.D. Peccei, and T. Yanagida, Nucl. Phys. **B279**, 401 (1987).
 14. J.E. Kim, Phys. Rev. Lett. **43**, 103 (1979);
M.A. Shifman, A.I. Vainstein, and V.I. Zakharov, Nucl. Phys. **B166**, 493 (1980).
 15. M. Dine, W. Fischler, and M. Srednicki, Phys. Lett. **B104**, 199 (1981);
A.R. Zhitnitsky, Sov. J. Nucl. Phys. **31**, 260 (1980).
 16. S.L. Cheng, C.Q. Geng, and W.T. Ni, Phys. Rev. **D52**, 3132 (1995).
 17. G. Raffelt and D. Seckel, Phys. Rev. Lett. **60**, 1793 (1988);
M. Carena and R.D. Peccei, Phys. Rev. **D40**, 652 (1989);
K. Choi, K. Kang, and J.E. Kim, Phys. Rev. Lett. **62**, 849 (1989).
 18. V.Y. Alexakhin *et al.* (COMPASS Collab.), Phys. Lett. **B647**, 8 (2007).
 19. A. Airapetian *et al.* (HERMES Collab.), Phys. Rev. **D75**, 012007 (2007) and Erratum *ibid.*, **D76**, 039901 (2007).
 20. J.R. Ellis and M. Karliner, in: *The spin structure of the nucleon: International school of nucleon structure* (3–10 August 1995, Erice, Italy), ed. by B. Frois, V.W. Hughes, and N. De Groot (World Scientific, Singapore, 1997) [hep-ph/9601280].
 21. S. Chang and K. Choi, Phys. Lett. **B316**, 51 (1993).
 22. D.A. Dicus *et al.*, Phys. Rev. **D18**, 1829 (1978).
 23. G. Raffelt and L. Stodolsky, Phys. Rev. **D37**, 1237 (1988).
 24. K. van Bibber *et al.*, Phys. Rev. Lett. **59**, 759 (1987).
 25. G. Ruoso *et al.*, Z. Phys. **C56**, 505 (1992);
R. Cameron *et al.*, Phys. Rev. **D47**, 3707 (1993).
 26. M. Fouche *et al.*, Phys. Rev. **D78**, 032013 (2008);
A.S. Chou *et al.* (GammeV Collab.), Phys. Rev. Lett. **100**, 080402 (2008);
A. Afanasev *et al.*, Phys. Rev. Lett. **101**, 120401 (2008);
K. Ehret *et al.* (ALPS Collab.), Nucl. Instrum. Methods **A612**, 83 (2009).
 27. P. Sikivie, D. Tanner, and K. van Bibber, Phys. Rev. Lett. **98**, 172002 (2007);
G. Mueller *et al.*, Phys. Rev. **D80**, 072004 (2009).
 28. A. Melissinos, Phys. Rev. Lett. **102**, 202001 (2009).
 29. L. Maiani *et al.*, Phys. Lett. **B175**, 359 (1986).
 30. Y. Semertzidis *et al.*, Phys. Rev. Lett. **64**, 2988 (1990).
 31. E. Zavattini *et al.* (PVLAS Collab.), Phys. Rev. Lett. **96**, 110406 (2006).
 32. E. Zavattini *et al.* (PVLAS Collab.), Phys. Rev. **D77**, 032006 (2008).
 33. E. Fischbach and C. Talmadge, Nature **356**, 207 (1992).
 34. J.E. Moody and F. Wilczek, Phys. Rev. D **30**, 130(1984);
A.N. Youdin *et al.*, Phys. Rev. Lett. **77**, 2170 (1996);
Wei-Tou Ni *et al.*, Phys. Rev. Lett. **82**, 2439 (1999);
D.F. Phillips *et al.*, Phys. Rev. **D63**, 111101 (R)(2001);
B.R. Heckel *et al.* (Eöt-Wash Collab.), Phys. Rev. Lett. **97**, 021603 (2006).
 35. M.S. Turner, Phys. Reports **197**, 67 (1990);
G.G. Raffelt, Phys. Reports **198**, 1 (1990).
 36. G.G. Raffelt, *Stars as Laboratories for Fundamental Physics*, (Univ. of Chicago Press, Chicago, 1996).
 37. G.G. Raffelt, Lect. Notes Phys. **741**, 51 (2008).
 38. P. Gondolo and G. Raffelt, Phys. Rev. **D79**, 107301 (2009).
 39. H. Schlattl, A. Weiss, and G. Raffelt, Astropart. Phys. **10**, 353 (1999).
 40. G. Raffelt and A. Weiss, Phys. Rev. **D51**, 1495 (1995);
M. Catelan, J.A. de Freitas Pacheco, and J.E. Horvath, Astrophys. J. **461**, 231 (1996).
 41. G.G. Raffelt, Phys. Lett. **B166**, 402 (1986);
S.I. Blinnikov and N.V. Dunina-Barkovskaya, Mon. Not. R. Astron. Soc. **266**, 289 (1994);
J. Isern *et al.*, J. Phys. Conf. Ser. **172**, 012005 (2009).
 42. A.H. Córdoba *et al.*, New Astron. **6**, 197 (2001);
J. Isern and E. García-Berro, Nucl. Phys. B Proc. Suppl. **114**, 107 (2003).
 43. J. Engel, D. Seckel, and A.C. Hayes, Phys. Rev. Lett. **65**, 960 (1990).
 44. T. Moroi and H. Murayama, Phys. Lett. **B440**, 69 (1998).
 45. K. van Bibber *et al.*, Phys. Rev. **D39**, 2089 (1989).
 46. D. Lazarus *et al.*, Phys. Rev. Lett. **69**, 2333 (1992).
 47. S. Moriyama *et al.*, Phys. Lett. **B434**, 147 (1998);
Y. Inoue *et al.*, Phys. Lett. **B536**, 18 (2002).
 48. M. Minowa *et al.*, Phys. Lett. **B668**, 93 (2008).
 49. S. Andriamonje *et al.* (CAST Collab.), JCAP **0704**, 010 (2007).
 50. E. Arik *et al.* (CAST Collab.), JCAP **0902**, 008 (2009).
 51. F.T. Avignone III *et al.*, Phys. Rev. Lett. **81**, 5068 (1998);
A. Morales *et al.* (COSME Collab.), Astropart. Phys. **16**, 325 (2002);
R. Bernabei *et al.*, Phys. Lett. **B515**, 6 (2001);
Z. Ahmed *et al.* (CDMS Collab.), Phys. Rev. Lett. **103**, 141802 (2009).
 52. H. Davoudiasl and P. Huber, Phys. Rev. Lett. **97**, 141302 (2006).
 53. J.W. Brockway, E.D. Carlson, and G.G. Raffelt, Phys. Lett. **B383**, 439 (1996);
J.A. Grifols, E. Massó, and R. Toldrà, Phys. Rev. Lett. **77**, 2372 (1996).
 54. C. Csaki, N. Kaloper, and J. Terning, Phys. Rev. Lett. **88**, 161302 (2002).
 55. A. Mirizzi, G.G. Raffelt, and P.D. Serpico, Lect. Notes Phys. **741**, 115 (2008).
 56. C. Burrage, A.C. Davis and D.J. Shaw, Phys. Rev. Lett. **102**, 201101 (2009).
 57. D. Hooper and P.D. Serpico, Phys. Rev. Lett. **99**, 231102 (2007);
K.A. Hochmuth and G. Sigl, Phys. Rev. **D76**, 123011 (2007);
A. De Angelis, O. Mansutti and M. Roncadelli, Phys. Rev. **D76**, 121301 (2007);
A. Mirizzi and D. Montanino, JCAP **0912**, 004 (2009).
 58. M.S. Turner, Phys. Rev. Lett. **59**, 2489 (1987) and Erratum *ibid.*, **60**, 1101 (1988);
E. Massó, F. Rota, and G. Zsembinszki, Phys. Rev. **D66**, 023004 (2002).

Gauge & Higgs Boson Particle Listings

Axions (A^0) and Other Very Light Bosons

59. A. Melchiorri, O. Mena, and A. Slosar, Phys. Rev. **D76**, 041303 (2007);
S. Hannestad *et al.*, JCAP **0804**, 019 (2008).
60. E. Massó and R. Toldra, Phys. Rev. **D55**, 7967 (1997).
61. J. Preskill, M.B. Wise, and F. Wilczek, Phys. Lett. **B120**, 127 (1983);
L.F. Abbott and P. Sikivie, Phys. Lett. **B120**, 133 (1983);
M. Dine and W. Fischler, Phys. Lett. **B120**, 137 (1983).
62. P. Sikivie, Lect. Notes Phys. **741**, 19 (2008).
63. M. Tegmark *et al.*, Phys. Rev. **D73**, 023505 (2006).
64. M. Beltrán, J. García-Bellido, and J. Lesgourgues, Phys. Rev. **D75**, 103507 (2007);
M.P. Hertzberg, M. Tegmark and F. Wilczek, Phys. Rev. **D78**, 083507 (2008);
J. Hamann *et al.*, JCAP **0906**, 022 (2009).
65. E.W. Kolb and I.I. Tkachev, Phys. Rev. Lett. **71**, 3051 (1993), Astrophys. J. **460**, L25 (1996).
66. M. Bershadsky *et al.*, Phys. Rev. Lett. **66**, 1398 (1991);
M. Ressel, Phys. Rev. **D44**, 3001 (1991).
67. D. Grin *et al.*, Phys. Rev. **D75**, 105018 (2007).
68. B.D. Blout *et al.*, Astrophys. J. **546**, 825 (2001).
69. P. Sikivie, Phys. Rev. **D32**, 2988 (1985);
L. Krauss *et al.*, Phys. Rev. Lett. **55**, 1797 (1985);
R. Bradley *et al.*, Rev. Mod. Phys. **75**, 777 (2003).
70. P. Sikivie and J. Ipser, Phys. Lett. **B291**, 288 (1992);
P. Sikivie *et al.*, Phys. Rev. Lett. **75**, 2911 (1995).
71. S. DePañfilis *et al.*, Phys. Rev. Lett. **59**, 839 (1987);
W. Wuensch *et al.*, Phys. Rev. **D40**, 3153 (1989);
C. Hagmann *et al.*, Phys. Rev. **D42**, 1297 (1990).
72. S. Asztalos *et al.*, Phys. Rev. **D69**, 011101 (2004).
73. L. Duffy *et al.*, Phys. Rev. Lett. **95**, 091304 (2005).
74. S. J. Asztalos *et al.* (ADMX Collab.), arXiv:0910.5914.
75. M. Mück, J.B. Kycia, and J. Clarke, Appl. Phys. Lett. **78**, 967 (2001).
76. I. Ogawa, S. Matsuki, and K. Yamamoto, Phys. Rev. **D53**, 1740 (1996).
77. S. Matsuki *et al.*, Nucl. Phys. B (Proc. Suppl.) **51**, 213 (1996);
Y. Kishimoto *et al.*, Phys. Lett. **A303**, 279 (2002);
M. Tada *et al.*, Phys. Lett. **A303**, 285 (2002).

A^0 (Axion) MASS LIMITS from Astrophysics and Cosmology

These bounds depend on model-dependent assumptions (i.e. — on a combination of axion parameters).

VALUE (MeV)	DOCUMENT ID	TECN.	COMMENT
•••	We do not use the following data for averages, fits, limits, etc. •••		
>0.2	BARROSO	82 ASTR	Standard Axion
>0.25	1 RAFFELT	82 ASTR	Standard Axion
>0.2	2 DICUS	78c ASTR	Standard Axion
	MIKHAELIAN	78 ASTR	Stellar emission
>0.3	2 SATO	78 ASTR	Standard Axion
>0.2	VYSOTSKII	78 ASTR	Standard Axion

¹ Lower bound from 5.5 MeV γ -ray line from the sun.

² Lower bound from requiring the red giants' stellar evolution not be disrupted by axion emission.

A^0 (Axion) and Other Light Boson (X^0) Searches in Hadron Decays

Limits are for branching ratios.

VALUE	CL%	DOCUMENT ID	TECN.	COMMENT
•••	We do not use the following data for averages, fits, limits, etc. •••			

$<2.4 \times 10^{-7}$	90	³ TUNG	09	K391	$K_L^0 \rightarrow \pi^0 \pi^0 A^0, A^0 \rightarrow \gamma\gamma$
		⁴ PARK	05	HYCP	$\Sigma^+ \rightarrow p A^0, A^0 \rightarrow \mu^+ \mu^-$
$<7 \times 10^{-10}$	90	⁵ ADLER	04	B787	$K^+ \rightarrow \pi^+ X^0$
$<7.3 \times 10^{-11}$	90	⁶ ANISIMOVSK.	04	B949	$K^+ \rightarrow \pi^+ X^0$
$<4.5 \times 10^{-11}$	90	⁷ ADLER	02c	B787	$K^+ \rightarrow \pi^+ X^0$
$<4 \times 10^{-5}$	90	⁸ ADLER	01	B787	$K^+ \rightarrow \pi^+ \pi^0 A^0$
$<4.9 \times 10^{-5}$	90	AMMAR	01b	CLEO	$B^\pm \rightarrow \pi^\pm (K^\pm) X^0$
$<5.3 \times 10^{-5}$	90	AMMAR	01b	CLEO	$B^0 \rightarrow K_S^0 X^0$
$<3.3 \times 10^{-5}$	90	⁹ ALTEGOER	98	NOMD	$\pi^0 \rightarrow \gamma X^0, m_{X^0} < 120$ MeV
$<5.0 \times 10^{-8}$	90	¹⁰ KITCHING	97	B787	$K^+ \rightarrow \pi^+ X^0 (X^0 \rightarrow \gamma\gamma)$
$<5.2 \times 10^{-10}$	90	¹¹ ADLER	96	B787	$K^+ \rightarrow \pi^+ X^0$
$<2.8 \times 10^{-4}$	90	¹² AMSLER	96b	CBAR	$\pi^0 \rightarrow \gamma X^0, m_{X^0} < 65$ MeV
$<3 \times 10^{-4}$	90	¹² AMSLER	96b	CBAR	$\eta \rightarrow \gamma X^0, m_{X^0} = 50-200$ MeV
$<4 \times 10^{-5}$	90	¹² AMSLER	96b	CBAR	$\eta' \rightarrow \gamma X^0, m_{X^0} = 50-925$ MeV
$<6 \times 10^{-5}$	90	¹² AMSLER	94b	CBAR	$\pi^0 \rightarrow \gamma X^0, m_{X^0} = 65-125$ MeV
$<6 \times 10^{-5}$	90	¹² AMSLER	94b	CBAR	$\eta \rightarrow \gamma X^0, m_{X^0} = 200-525$ MeV
$<7 \times 10^{-3}$	90	¹³ MEIJERDREES	94	CNTR	$\pi^0 \rightarrow \gamma X^0, m_{X^0} = 25$ MeV
$<2 \times 10^{-3}$	90	¹³ MEIJERDREES	94	CNTR	$\pi^0 \rightarrow \gamma X^0, m_{X^0} = 100$ MeV
$<2 \times 10^{-7}$	90	¹⁴ ATIYA	93b	B787	Sup. by ADLER 04
$<3 \times 10^{-13}$	90	¹⁵ NG	93	COSM	$\pi^0 \rightarrow \gamma X^0$
$<1.1 \times 10^{-8}$	90	¹⁶ ALLIEGRO	92	SPEC	$K^+ \rightarrow \pi^+ X^0 (X^0 \rightarrow e^+ e^-)$
$<5 \times 10^{-4}$	90	¹⁷ ATIYA	92	B787	$\pi^0 \rightarrow \gamma X^0$
$<4 \times 10^{-6}$	90	¹⁸ MEIJERDREES	92	SPEC	$\pi^0 \rightarrow \gamma X^0, X^0 \rightarrow e^+ e^-, m_{X^0} = 100$ MeV
$<1 \times 10^{-7}$	90	¹⁹ ATIYA	90b	B787	Sup. by KITCHING 97
$<1.3 \times 10^{-8}$	90	²⁰ KORENCHENKO	87	SPEC	$\pi^+ \rightarrow e^+ \nu A^0 (A^0 \rightarrow e^+ e^-)$
$<1 \times 10^{-9}$	90	²¹ EICHLER	86	SPEC	Stopped $\pi^+ \rightarrow e^+ \nu A^0$
$<2 \times 10^{-5}$	90	²² YAMAZAKI	84	SPEC	For $160 < m < 260$ MeV
$<(1.5-4) \times 10^{-6}$	90	²² YAMAZAKI	84	SPEC	K decay, $m_{X^0} \ll 100$ MeV
		²³ ASANO	82	CNTR	Stopped $K^+ \rightarrow \pi^+ X^0$
		²⁴ ASANO	81b	CNTR	Stopped $K^+ \rightarrow \pi^+ X^0$
		²⁵ ZHITNITSKII	79		Heavy axion

³ The limit applies at $m_{A^0} = 214.3$ MeV, motivated by PARK 05. TUNG 09 show mass-dependent limits in their Fig. 5.

⁴ PARK 05 found three candidate events for $\Sigma^+ \rightarrow p \mu^+ \mu^-$ in the HyperCP experiment. Due to a narrow spread in dimuon mass, they hypothesize the events as a possible signal of a new boson. It can be interpreted as an axion-like particle with $m_{A^0} = 214.3 \pm 0.5$ MeV and the branching fraction $B(\Sigma^+ \rightarrow p A^0) \times B(A^0 \rightarrow \mu^+ \mu^-) = (3.1^{+2.4}_{-1.9} \times 1.5) \times 10^{-8}$.

⁵ This limit applies for a mass near 180 MeV. For other masses in the range $m_{X^0} = 150-250$ MeV the limit is less restrictive, but still improves ADLER 02c and ATIYA 93b.

⁶ ANISIMOVSKY 04 bound is for $m_{X^0} = 0$.

⁷ ADLER 02c bound is for $m_{X^0} < 60$ MeV. See Fig. 2 for limits at higher masses.

⁸ The quoted limit is for $m_{X^0} = 0-80$ MeV. See their Fig. 5 for the limit at higher mass. The branching fraction limit assumes pure phase space decay distributions.

⁹ ALTEGOER 98 looked for X^0 from π^0 decay which penetrate the shielding and convert to π^0 in the external Coulomb field of a nucleus.

¹⁰ KITCHING 97 limit is for $B(K^+ \rightarrow \pi^+ X^0) \cdot B(X^0 \rightarrow \gamma\gamma)$ and applies for $m_{X^0} \approx 50$ MeV, $\tau_{X^0} < 10^{-10}$ s. Limits are provided for $0 < m_{X^0} < 100$ MeV, $\tau_{X^0} < 10^{-8}$ s.

¹¹ ADLER 96 looked for a peak in missing-mass distribution. This work is an update of ATIYA 93. The limit is for massless stable X^0 particles and extends to $m_{X^0} = 80$ MeV at the same level. See paper for dependence on finite lifetime.

¹² AMSLER 94b and AMSLER 96b looked for a peak in missing-mass distribution.

¹³ The MEIJERDREES 94 limit is based on inclusive photon spectrum and is independent of X^0 decay modes. It applies to $\tau(X^0) > 10^{-23}$ sec.

¹⁴ ATIYA 93b looked for a peak in missing mass distribution. The bound applies for stable X^0 of $m_{X^0} = 150-250$ MeV, and the limit becomes stronger (10^{-8}) for $m_{X^0} = 180-240$ MeV.

¹⁵ NG 93 studied the production of X^0 via $\gamma\gamma \rightarrow \pi^0 \rightarrow \gamma X^0$ in the early universe at $T \approx 1$ MeV. The bound on extra neutrinos from nucleosynthesis $\Delta N_\nu < 0.3$ (WALKER 91) is employed. It applies to $m_{X^0} \ll 1$ MeV in order to be relativistic down to nucleosynthesis temperature. See paper for heavier X^0 .

¹⁶ ALLIEGRO 92 limit applies for $m_{X^0} = 150-340$ MeV and is the branching ratio times the decay probability. Limit is $< 1.5 \times 10^{-8}$ at 99% CL.

¹⁷ ATIYA 92 looked for a peak in missing mass distribution. The limit applies to $m_{X^0} = 0-130$ MeV in the narrow resonance limit. See paper for the dependence on lifetime. Covariance requires X^0 to be a vector particle.

¹⁸ MEIJERDREES 92 limit applies for $\tau_{X^0} = 10^{-23}-10^{-11}$ sec. Limits between 2×10^{-4} and 4×10^{-6} are obtained for $m_{X^0} = 25-120$ MeV. Angular momentum conservation requires that X^0 has spin ≥ 1 .

¹⁹ ATIYA 90b limit is for $B(K^+ \rightarrow \pi^+ X^0) \cdot B(X^0 \rightarrow \gamma\gamma)$ and applies for $m_{X^0} = 50$ MeV, $\tau_{X^0} < 10^{-10}$ s. Limits are also provided for $0 < m_{X^0} < 100$ MeV, $\tau_{X^0} < 10^{-8}$ s.

²⁰ KORENCHENKO 87 limit assumes $m_{A^0} = 1.7$ MeV, $\tau_{A^0} \lesssim 10^{-12}$ s, and $B(A^0 \rightarrow e^+ e^-) = 1$.

²¹ EICHLER 86 looked for $\pi^+ \rightarrow e^+ \nu A^0$ followed by $A^0 \rightarrow e^+ e^-$. Limits on the branching fraction depend on the mass and lifetime of A^0 . The quoted limits are valid when $\tau(A^0) \gtrsim 3 \times 10^{-10}$ s if the decays are kinematically allowed.

²² YAMAZAKI 84 looked for a discrete line in $K^+ \rightarrow \pi^+ X$. Sensitive to wide mass range (5-300 MeV), independent of whether X decays promptly or not.

See key on page 405

Gauge & Higgs Boson Particle Listings

Axions (A^0) and Other Very Light Bosons

²³ASANO 82 at KEK set limits for $B(K^+ \rightarrow \pi^+ X^0)$ for $m_{X^0} < 100$ MeV as BR $< 4 \times 10^{-8}$ for $\tau(X^0 \rightarrow n\gamma's) > 1 \times 10^{-9}$ s, BR $< 1.4 \times 10^{-6}$ for $\tau < 1 \times 10^{-9}$ s.
²⁴ASANO 81B is KEK experiment. Set $B(K^+ \rightarrow \pi^+ X^0) < 3.8 \times 10^{-8}$ at CL = 90%.
²⁵ZHITNITSKII 79 argue that a heavy axion predicted by YANG 78 ($3 < m < 40$ MeV) contradicts experimental muon anomalous magnetic moments.

A^0 (Axion) Searches in Quarkonium Decays

Decay or transition of quarkonium. Limits are for branching ratio.

VALUE	CL%	DOCUMENT ID	TECN	COMMENT
● ● ● We do not use the following data for averages, fits, limits, etc. ● ● ●				
		²⁶ AUBERT 09Z	BABR	$\Upsilon(2S, 3S) \rightarrow \gamma A^0, A^0 \rightarrow \mu^+ \mu^-$
		²⁷ LOVE 08	CLEO	$\Upsilon(1S) \rightarrow \gamma A^0, A^0 \rightarrow \mu^+ \mu^-,$ or $\tau^+ \tau^-$
$< 1.3 \times 10^{-5}$	90	²⁸ BALEST 95	CLEO	$\Upsilon(1S) \rightarrow A^0 \gamma$
$< 4.0 \times 10^{-5}$	90	ANTREASYAN 90C	CBAL	$\Upsilon(1S) \rightarrow A^0 \gamma$
		ANTREASYAN 90C	RVUE	
$< 5 \times 10^{-5}$	90	³⁰ DRUZHININ 87	ND	$\phi \rightarrow A^0 \gamma (A^0 \rightarrow e^+ e^-)$
$< 2 \times 10^{-3}$	90	³¹ DRUZHININ 87	ND	$\phi \rightarrow A^0 \gamma (A^0 \rightarrow \gamma \gamma)$
$< 7 \times 10^{-6}$	90	³² DRUZHININ 87	ND	$\phi \rightarrow A^0 \gamma (A^0 \rightarrow \text{missing})$
$< 3.1 \times 10^{-4}$	90	³³ ALBRECHT 86D	ARG	$\Upsilon(1S) \rightarrow A^0 \gamma (A^0 \rightarrow e^+ e^-)$
$< 4 \times 10^{-4}$	90	³³ ALBRECHT 86D	ARG	$\Upsilon(1S) \rightarrow A^0 \gamma (A^0 \rightarrow \mu^+ \mu^-,$ $\pi^+ \pi^-, K^+ K^-)$
$< 8 \times 10^{-4}$	90	³⁴ ALBRECHT 86D	ARG	$\Upsilon(1S) \rightarrow A^0 \gamma$
$< 1.3 \times 10^{-3}$	90	³⁵ ALBRECHT 86D	ARG	$\Upsilon(1S) \rightarrow A^0 \gamma (A^0 \rightarrow e^+ e^-,$ $\gamma \gamma)$
$< 2 \times 10^{-3}$	90	³⁶ BOWCOCK 86	CLEO	$\Upsilon(2S) \rightarrow \Upsilon(1S) \rightarrow A^0$
$< 5 \times 10^{-3}$	90	³⁷ MAGERAS 86	CUSB	$\Upsilon(1S) \rightarrow A^0 \gamma$
$< 3 \times 10^{-4}$	90	³⁸ ALAM 83	CLEO	$\Upsilon(1S) \rightarrow A^0 \gamma$
$< 9.1 \times 10^{-4}$	90	³⁹ NICZYPORUK 83	LENA	$\Upsilon(1S) \rightarrow A^0 \gamma$
$< 1.4 \times 10^{-5}$	90	⁴⁰ EDWARDS 82	CBAL	$J/\psi \rightarrow A^0 \gamma$
$< 3.5 \times 10^{-4}$	90	⁴¹ SIVERTZ 82	CUSB	$\Upsilon(1S) \rightarrow A^0 \gamma$
$< 1.2 \times 10^{-4}$	90	⁴¹ SIVERTZ 82	CUSB	$\Upsilon(3S) \rightarrow A^0 \gamma$

²⁶AUBERT 09Z show mass-dependent limits on $B(\Upsilon \rightarrow \gamma A^0) B(A^0 \rightarrow \mu^+ \mu^-)$ in their Fig. 2.
²⁷LOVE 08 show mass-dependent limits on $B(\Upsilon \rightarrow \gamma A^0) B(A^0 \rightarrow \mu^+ \mu^-)$ or $\tau^+ \tau^-$ on their Fig. 3.

²⁸BALEST 95 looked for a monochromatic γ from $\Upsilon(1S)$ decay. The bound is for $m_{A^0} < 5.0$ GeV. See Fig. 7 in the paper for bounds for heavier m_{A^0} . They also quote a bound on branching ratios $10^{-3}-10^{-5}$ of three-body decay $\gamma X \bar{X}$ for $0 < m_X < 3.1$ GeV.

²⁹The combined limit of ANTREASYAN 90C and EDWARDS 82 excludes standard axion with $m_{A^0} < 2m_e$ at 90% CL as long as $C_\Upsilon C_{J/\psi} > 0.09$, where $C_V (V = \Upsilon, J/\psi)$ is the reduction factor for $\Gamma(V \rightarrow A^0 \gamma)$ due to QCD and/or relativistic corrections. The same data excludes $0.02 < x < 260$ (90% CL) if $C_\Upsilon = C_{J/\psi} = 0.5$, and further combining with ALBRECHT 86D result excludes $5 \times 10^{-5} < x < 260$. x is the ratio of the vacuum expectation values of the two Higgs fields. These limits use conventional assumption $\Gamma(A^0 \rightarrow ee) \propto x^{-2}$. The alternative assumption $\Gamma(A^0 \rightarrow ee) \propto x^2$ gives a somewhat different excluded region $0.00075 < x < 44$.

³⁰The first DRUZHININ 87 limit is valid when $\tau_{A^0}/m_{A^0} < 3 \times 10^{-13}$ s/MeV and $m_{A^0} < 20$ MeV.

³¹The second DRUZHININ 87 limit is valid when $\tau_{A^0}/m_{A^0} < 5 \times 10^{-13}$ s/MeV and $m_{A^0} < 20$ MeV.

³²The third DRUZHININ 87 limit is valid when $\tau_{A^0}/m_{A^0} > 7 \times 10^{-12}$ s/MeV and $m_{A^0} < 200$ MeV.

³³ $\tau_{A^0} < 1 \times 10^{-13}$ s and $m_{A^0} < 1.5$ GeV. Applies for $A^0 \rightarrow \gamma \gamma$ when $m_{A^0} < 100$ MeV.

³⁴ $\tau_{A^0} > 1 \times 10^{-7}$ s.

³⁵Independent of τ_{A^0} .

³⁶BOWCOCK 86 looked for A^0 that decays into $e^+ e^-$ in the cascade decay $\Upsilon(2S) \rightarrow \Upsilon(1S) \pi^+ \pi^-$ followed by $\Upsilon(1S) \rightarrow A^0 \gamma$. The limit for $B(\Upsilon(1S) \rightarrow A^0 \gamma) B(A^0 \rightarrow e^+ e^-)$ depends on m_{A^0} and τ_{A^0} . The quoted limit for $m_{A^0} = 1.8$ MeV is at $\tau_{A^0} \sim 2 \times 10^{-12}$ s, where the limit is the worst. The same limit 2×10^{-3} applies for all lifetimes for masses $2m_e < m_{A^0} < 2m_\mu$ when the results of this experiment are combined with the results of ALAM 83.

³⁷MAGERAS 86 looked for $\Upsilon(1S) \rightarrow \gamma A^0 (A^0 \rightarrow e^+ e^-)$. The quoted branching fraction limit is for $m_{A^0} = 1.7$ MeV, at $\tau(A^0) \sim 4 \times 10^{-13}$ s where the limit is the worst.

³⁸ALAM 83 is at CESR. This limit combined with limit for $B(J/\psi \rightarrow A^0 \gamma)$ (EDWARDS 82) excludes standard axion.

³⁹NICZYPORUK 83 is DESY-DORIS experiment. This limit together with lower limit 9.2×10^{-4} of $B(\Upsilon \rightarrow A^0 \gamma)$ derived from $B(J/\psi(1S) \rightarrow A^0 \gamma)$ limit (EDWARDS 82) excludes standard axion.

⁴⁰EDWARDS 82 looked for $J/\psi \rightarrow \gamma A^0$ decays by looking for events with a single γ [of energy $\sim 1/2$ the $J/\psi(1S)$ mass], plus nothing else in the detector. The limit is inconsistent with the axion interpretation of the FAISSNER 81B result.

⁴¹SIVERTZ 82 is CESR experiment. Looked for $\Upsilon \rightarrow \gamma A^0, A^0$ undetected. Limit for $1S$ (3S) is valid for $m_{A^0} < 7$ GeV (4 GeV).

A^0 (Axion) Searches in Positronium Decays

Decay or transition of positronium. Limits are for branching ratio.

VALUE	CL%	DOCUMENT ID	TECN	COMMENT
● ● ● We do not use the following data for averages, fits, limits, etc. ● ● ●				

$< 4.4 \times 10^{-5}$	90	⁴² BADERT... 02	CNTR	$\alpha\text{-Ps} \rightarrow \gamma X_1 X_2, m_{X_1} + m_{X_2} \leq 900$ keV
$< 2 \times 10^{-4}$	90	MAENO 95	CNTR	$\alpha\text{-Ps} \rightarrow A^0 \gamma, m_{A^0} = 850-1013$ keV
$< 3.0 \times 10^{-3}$	90	⁴³ ASAI 94	CNTR	$\alpha\text{-Ps} \rightarrow A^0 \gamma, m_{A^0} = 30-500$ keV
$< 2.8 \times 10^{-5}$	90	⁴⁴ AKOPYAN 91	CNTR	$\alpha\text{-Ps} \rightarrow A^0 \gamma (A^0 \rightarrow \gamma \gamma),$ $m_{A^0} < 30$ keV
$< 1.1 \times 10^{-6}$	90	⁴⁵ ASAI 91	CNTR	$\alpha\text{-Ps} \rightarrow A^0 \gamma, m_{A^0} < 800$ keV
$< 3.8 \times 10^{-4}$	90	GNINENKO 90	CNTR	$\alpha\text{-Ps} \rightarrow A^0 \gamma, m_{A^0} < 30$ keV
$< (1-5) \times 10^{-4}$	95	⁴⁶ TSUCHIAKI 90	CNTR	$\alpha\text{-Ps} \rightarrow A^0 \gamma, m_{A^0} = 300-900$ keV
$< 6.4 \times 10^{-5}$	90	⁴⁷ ORITO 89	CNTR	$\alpha\text{-Ps} \rightarrow A^0 \gamma, m_{A^0} < 30$ keV
		⁴⁸ AMALDI 85	CNTR	Ortho-positronium
		⁴⁹ CARBONI 83	CNTR	Ortho-positronium

⁴²BADERTSCHER 02 looked for a three-body decay of ortho-positronium into a photon and two penetrating (neutral or milli-charged) particles.

⁴³The ASAI 94 limit is based on inclusive photon spectrum and is independent of A^0 decay modes.

⁴⁴The AKOPYAN 91 limit applies for a short-lived A^0 with $\tau_{A^0} < 10^{-13}$ s, m_{A^0} [keV].

⁴⁵ASAI 91 limit translates to $g_{A^0 e^+ e^-}^2 / 4\pi < 1.1 \times 10^{-11}$ (90% CL) for $m_{A^0} < 800$ keV.

⁴⁶The TSUCHIAKI 90 limit is based on inclusive photon spectrum and is independent of A^0 decay modes.

⁴⁷ORITO 89 limit translates to $g_{A^0 e^+ e^-}^2 / 4\pi < 6.2 \times 10^{-10}$. Somewhat more sensitive limits are obtained for larger m_{A^0} : $B < 7.6 \times 10^{-6}$ at 100 keV.

⁴⁸AMALDI 85 set limits $B(A^0 \gamma) / B(\gamma \gamma) < (1-5) \times 10^{-6}$ for $m_{A^0} = 900-100$ keV which are about 1/10 of the CARBONI 83 limits.

⁴⁹CARBONI 83 looked for ortho-positronium to $A^0 \gamma$. Set limit for A^0 electron coupling squared, $g(e e A^0)^2 / (4\pi) < 6 \times 10^{-10} \cdot 7 \times 10^{-9}$ for m_{A^0} from 150-900 keV (CL = 99.7%). This is about 1/10 of the bound from g_{-2} experiments.

A^0 (Axion) Search in Photoproduction

VALUE	CL%	DOCUMENT ID	TECN	COMMENT
● ● ● We do not use the following data for averages, fits, limits, etc. ● ● ●				
		⁵⁰ BASSOMPIERE... 95		$m_{A^0} = 1.8 \pm 0.2$ MeV

⁵⁰BASSOMPIERE 95 is an extension of BASSOMPIERE 93. They looked for a peak in the invariant mass of $e^+ e^-$ pairs in the region $m_{e^+ e^-} = 1.8 \pm 0.2$ MeV. They obtained bounds on the production rate A^0 for $\tau(A^0) = 10^{-18}-10^{-9}$ sec. They also found an excess of events in the range $m_{e^+ e^-} = 2.1-3.5$ MeV.

A^0 (Axion) Production in Hadron Collisions

Limits are for $\sigma(A^0) / \sigma(\pi^0)$.

VALUE	CL%	EVTS	DOCUMENT ID	TECN	COMMENT
● ● ● We do not use the following data for averages, fits, limits, etc. ● ● ●					
			⁵¹ JAIN 07	CNTR	$A^0 \rightarrow e^+ e^-$
			⁵² AHMAD 97	SPEC	e^+ production
			⁵³ LEINBERGER 97	SPEC	$A^0 \rightarrow e^+ e^-$
			⁵⁴ GANZ 96	SPEC	$A^0 \rightarrow e^+ e^-$
			⁵⁵ KAMEL 96	EMUL	^{32}S emulsion, $A^0 \rightarrow e^+ e^-$
			⁵⁶ BLUEMLEIN 92	BDMP	$A^0 N_Z \rightarrow \ell^+ \ell^- N_Z$
			⁵⁷ MEIJERDREES 92	SPEC	$\pi^- p \rightarrow n A^0, A^0 \rightarrow e^+ e^-$
			⁵⁸ BLUEMLEIN 91	BDMP	$A^0 \rightarrow e^+ e^-, 2\gamma$
			⁵⁹ FAISSNER 89	OSPK	Beam dump, $A^0 \rightarrow e^+ e^-$
			⁶⁰ DEBOER 88	RVUE	$A^0 \rightarrow e^+ e^-$
			⁶¹ EL-NADI 88	EMUL	$A^0 \rightarrow e^+ e^-$
			⁶² FAISSNER 88	OSPK	Beam dump, $A^0 \rightarrow 2\gamma$
			⁶³ BADIER 86	BDMP	$A^0 \rightarrow e^+ e^-$
$< 2 \times 10^{-11}$	90	0	⁶⁴ BERGSMA 85	CHRM	CERN beam dump
$< 1 \times 10^{-13}$	90	0	⁶⁴ BERGSMA 85	CHRM	CERN beam dump
		24	⁶⁵ FAISSNER 83	OSPK	Beam dump, $A^0 \rightarrow 2\gamma$
			⁶⁶ FAISSNER 83B	RVUE	LAMPF beam dump
			⁶⁷ FRANK 83B	RVUE	LAMPF beam dump
			⁶⁸ HOFFMAN 83	CNTR	$\pi p \rightarrow n A^0 (A^0 \rightarrow e^+ e^-)$
			⁶⁹ FETSCHER 82	RVUE	See FAISSNER 81B
		12	⁷⁰ FAISSNER 81	OSPK	CERN PS ν wideband
		15	⁷¹ FAISSNER 81B	OSPK	Beam dump, $A^0 \rightarrow 2\gamma$
		8	⁷² KIM 81	OSPK	26 GeV $p N \rightarrow A^0 X$
		0	⁷³ FAISSNER 80	OSPK	Beam dump, $A^0 \rightarrow e^+ e^-$
$< 1 \times 10^{-8}$	90		⁷⁴ JACQUES 80	HLBC	28 GeV protons
$< 1 \times 10^{-14}$	90		⁷⁴ JACQUES 80	HLBC	Beam dump
			⁷⁵ SOUKAS 80	CALO	28 GeV p beam dump
			⁷⁶ BECHIS 79	CNTR	
$< 1 \times 10^{-8}$	90		⁷⁷ COTEUS 79	OSPK	Beam dump
$< 1 \times 10^{-3}$	95		⁷⁸ DISHAW 79	CALO	400 GeV pp
$< 1 \times 10^{-8}$	90		ALIBRAN 78	HYBR	Beam dump
$< 6 \times 10^{-9}$	95		ASRATYAN 78B	CALO	Beam dump

Gauge & Higgs Boson Particle Listings

Axions (A^0) and Other Very Light Bosons

- $<1.5 \times 10^{-8}$ 90 79 BELLOTTI 78 HLBC Beam dump
 $<5.4 \times 10^{-14}$ 90 79 BELLOTTI 78 HLBC $m_{A^0}=1.5$ MeV
 $<4.1 \times 10^{-9}$ 90 79 BELLOTTI 78 HLBC $m_{A^0}=1$ MeV
 $<1. \times 10^{-8}$ 90 80 BOSETTI 78B HYBR Beam dump
 81 DONNELLY 78
 $<0.5 \times 10^{-8}$ 90 HANSL 78D WIRE Beam dump
 82 MICELMAC... 78
 83 VYSOTSKII 78
- 51 JAIN 07 claims evidence for $A^0 \rightarrow e^+e^-$ produced in ^{207}Pb collision on nuclear emulsion (Ag/Br) for $m(A^0) = 7 \pm 1$ or 19 ± 1 MeV and $\tau(A^0) \leq 10^{-13}$ s.
 52 AHMAD 97 reports a result of APEX Collaboration which studied positron production in $^{238}\text{U} + ^{232}\text{Th}$ and $^{238}\text{U} + ^{181}\text{Ta}$ collisions, without requiring a coincident electron. No narrow lines were found for $250 < E_{e^+} < 750$ keV.
 53 LEINBERGER 97 (ORANGE Collaboration) at GSI looked for a narrow sum-energy e^+e^- line at ~ 635 keV in $^{238}\text{U} + ^{181}\text{Ta}$ collision. Limits on the production probability for a narrow sum-energy e^+e^- line are set. See their Table 2.
 54 GANZ 96 (EPOS II Collaboration) has placed upper bounds on the production cross section of e^+e^- pairs from $^{238}\text{U} + ^{181}\text{Ta}$ and $^{238}\text{U} + ^{232}\text{Th}$ collisions at GSI. See Table 2 for limits both for back-to-back and isotropic configurations of e^+e^- pairs. These limits rule out the existence of peaks in the e^+e^- sum-energy distribution, reported by an earlier version of this experiment.
 55 KAMEL 96 looked for e^+e^- pairs from the collision of ^{32}S (200 GeV/nucleon) and emulsion. No evidence of mass peaks is found in the region of sensitivity $m_{ee} > 2$ MeV.
 56 BLUEMLEIN 92 is a proton beam dump experiment at Serpukhov with a secondary target to induce Bethe-Heitler production of e^+e^- or $\mu^+\mu^-$ from the produce A^0 . See Fig. 5 for the excluded region in m_{A^0} - x plane. For the standard axion, $0.3 < x < 25$ is excluded at 95% CL. If combined with BLUEMLEIN 91, $0.008 < x < 32$ is excluded.
 57 MEIJERDREES 92 give $\Gamma(\pi^+p \rightarrow nA^0) \cdot \text{B}(A^0 \rightarrow e^+e^-) / \Gamma(\pi^+p \rightarrow \text{all}) < 10^{-5}$ (90% CL) for $m_{A^0} = 100$ MeV, $\tau_{A^0} = 10^{-11} - 10^{-23}$ sec. Limits ranging from 2.5×10^{-3} to 10^{-7} are given for $m_{A^0} = 25 - 136$ MeV.
 58 BLUEMLEIN 91 is a proton beam dump experiment at Serpukhov. No candidate event for $A^0 \rightarrow e^+e^-$, 2γ are found. Fig. 6 gives the excluded region in m_{A^0} - x plane ($x = \tan\beta = v_2/v_1$). Standard axion is excluded for $0.2 < m_{A^0} < 3.2$ MeV for most $x > 1$, $0.2 - 11$ MeV for most $x < 1$.
 59 FAISSNER 89 searched for $A^0 \rightarrow e^+e^-$ in a proton beam dump experiment at SIN. No excess of events was observed over the background. A standard axion with mass $2m_e - 20$ MeV is excluded. Lower limit on f_{A^0} of $\sim 10^4$ GeV is given for $m_{A^0} = 2m_e - 20$ MeV.
 60 DEBOER 88 reanalyze EL-NADI 88 data and claim evidence for three distinct states with mass ~ 1.1 , ~ 2.1 , and ~ 9 MeV, lifetimes $10^{-16} - 10^{-15}$ s decaying to e^+e^- and note the similarity of the data with those of a cosmic-ray experiment by Bristol group (B.M. Anand, Proc. of the Royal Society of London, Section A **A22** 183 (1953)). For a criticism see PERKINS 89, who suggests that the events are compatible with π^0 Dalitz decay. DEBOER 89b is a reply which contests the criticism.
 61 EL-NADI 88 claim the existence of a neutral particle decaying into e^+e^- with mass 1.60 ± 0.59 MeV, lifetime $(0.15 \pm 0.01) \times 10^{-14}$ s, which is produced in heavy ion interactions with emulsion nuclei at ~ 4 GeV/c/nucleon.
 62 FAISSNER 88 is a proton beam dump experiment at SIN. They found no candidate event for $A^0 \rightarrow \gamma\gamma$. A standard axion decaying to 2γ is excluded except for a region $x \approx 1$. Lower limit on f_{A^0} of $10^2 - 10^3$ GeV is given for $m_{A^0} = 0.1 - 1$ MeV.
 63 BADIER 86 did not find long-lived A^0 in 300 GeV π^- Beam Dump Experiment that decays into e^+e^- in the mass range $m_{A^0} = (20 - 200)$ MeV, which excludes the A^0 decay constant $f(A^0)$ in the interval (60-600) GeV. See their figure 6 for excluded region on $f(A^0)$ - m_{A^0} plane.
 64 BERGSMAN 85 look for $A^0 \rightarrow 2\gamma, e^+e^-, \mu^+\mu^-$. First limit above is for $m_{A^0} = 1$ MeV; second is for 200 MeV. See their figure 4 for excluded region on $f_{A^0} - m_{A^0}$ plane, where f_{A^0} is A^0 decay constant. For Peccei-Quinn PECCCI 77 $A^0, m_{A^0} < 180$ keV and $\tau > 0.037$ s. (CL = 90%). For the axion of FAISSNER 81b at 250 keV, BERGSMAN 85 expect 15 events but observe zero.
 65 FAISSNER 83 observed 19 $1-\gamma$ and 12 $2-\gamma$ events where a background of 4.8 and 2.3 respectively is expected. A small-angle peak is observed even if iron wall is set in front of the decay region.
 66 FAISSNER 83b extrapolate SIN γ signal to LAMPF ν experimental condition. Resulting 370 γ 's are not at variance with LAMPF upper limit of 450 γ 's. Derived from LAMPF limit that $[d\sigma(A^0)/d\omega \text{ at } 90^\circ] m_{A^0} / \tau_{A^0} < 14 \times 10^{-35} \text{ cm}^2 \text{ sr}^{-1} \text{ MeV ms}^{-1}$. See comment on FRANK 83b.
 67 FRANK 83b stress the importance of LAMPF data bins with negative net signal. By statistical analysis say that LAMPF and SIN-A0 are at variance when extrapolation by phase-space model is done. They find LAMPF upper limit is 248 not 450 γ 's. See comment on FAISSNER 83b.
 68 HOFFMAN 83 set CL = 90% limit $d\sigma/dt \text{ B}(e^+e^-) < 3.5 \times 10^{-32} \text{ cm}^2/\text{GeV}^2$ for $140 < m_{A^0} < 160$ MeV. Limit assumes $\tau(A^0) < 10^{-9}$ s.
 69 FETSCHER 82 reanalyzes SIN beam-dump data of FAISSNER 81. Claims no evidence for axion since $2-\gamma$ peak rate remarkably decreases if iron wall is set in front of the decay region.
 70 FAISSNER 81 see excess μe events. Suggest axion interactions.
 71 FAISSNER 81b is SIN 590 MeV proton beam dump. Observed 14.5 ± 5.0 events of 2γ decay of long-lived neutral penetrating particle with $m_{2\gamma} \lesssim 1$ MeV. Axion interpretation with η - A^0 mixing gives $m_{A^0} = 250 \pm 25$ keV, $\tau(2\gamma) = (7.3 \pm 3.7) \times 10^{-3}$ s from above rate. See critical remarks below in comments of FETSCHER 82, FAISSNER 83, FAISSNER 83b, FRANK 83b, and BERGSMAN 85. Also see in the next subsection ALEKSEEV 82b, CAVAIGNAC 83, and ANANEV 85.
 72 KIM 81 analyzed 8 candidates for $A^0 \rightarrow 2\gamma$ obtained by Aachen-Padova experiment at CERN with 26 GeV protons on Be. Estimated axion mass is about 300 keV and lifetime is $(0.86 - 5.6) \times 10^{-3}$ s depending on models. Faissner (private communication), says axion production underestimated and mass overestimated. Correct value around 200 keV.

- 73 FAISSNER 80 is SIN beam dump experiment with 590 MeV protons looking for $A^0 \rightarrow e^+e^-$ decay. Assuming $A^0/\pi^0 = 5.5 \times 10^{-7}$, obtained decay rate limit $20/(A^0 \text{ mass}) \text{ MeV/s}$ (CL = 90%), which is about 10^{-7} below theory and interpreted as upper limit to $m_{A^0} < 2m_e$.
 74 JACQUES 80 is a BNL beam dump experiment. First limit above comes from nonobservation of excess neutral-current-type events [$\sigma(\text{production})\sigma(\text{interaction}) < 7. \times 10^{-68} \text{ cm}^4$, CL = 90%]. Second limit is from nonobservation of axion decays into 2γ 's or e^+e^- , and for axion mass a few MeV.
 75 SOUKAS 80 at BNL observed no excess of neutral-current-type events in beam dump.
 76 BECHIS 79 looked for the axion production in low energy electron Bremsstrahlung and the subsequent decay into either 2γ or e^+e^- . No signal found. CL = 90% limits for model parameter(s) are given.
 77 COTEUS 79 is a beam dump experiment at BNL.
 78 DISHAW 79 is a calorimetric experiment and looks for low energy tail of energy distributions due to energy lost to weakly interacting particles.
 79 BELLOTTI 78 first value comes from search for $A^0 \rightarrow e^+e^-$. Second value comes from search for $A^0 \rightarrow 2\gamma$, assuming mass $< 2m_e$. For any mass satisfying this, limit is above value $\times (\text{mass})^{-4}$. Third value uses data of PL 60B 401 and quotes $\sigma(\text{production})\sigma(\text{interaction}) < 10^{-67} \text{ cm}^4$.
 80 BOSETTI 78B quotes $\sigma(\text{production})\sigma(\text{interaction}) < 2. \times 10^{-67} \text{ cm}^4$.
 81 DONNELLY 78 examines data from reactor neutrino experiments of REINES 76 and GURR 74 as well as SLAC beam dump experiment. Evidence is negative.
 82 MICELMACHER 78 finds no evidence of axion existence in reactor experiments of REINES 76 and GURR 74. (See reference under DONNELLY 78 below).
 83 VYSOTSKII 78 derived lower limit for the axion mass 25 keV from luminosity of the sun and 200 keV from red supergiants.

A^0 (Axion) Searches in Reactor Experiments

VALUE	DOCUMENT ID	TECN	COMMENT
• • • We do not use the following data for averages, fits, limits, etc. • • •			
	84 CHANG 07		Primakoff or Compton
	85 ALTMANN 95	CNTR	Reactor; $A^0 \rightarrow e^+e^-$
	86 KETOV 86	SPEC	Reactor; $A^0 \rightarrow \gamma\gamma$
	87 KOCH 86	SPEC	Reactor; $A^0 \rightarrow \gamma\gamma$
	88 DATAR 82	CNTR	Light water reactor
	89 VUILLEUMIER 81	CNTR	Reactor; $A^0 \rightarrow 2\gamma$
84 CHANG 07 looked for monochromatic photons from Primakoff or Compton conversion of axions from the Kuo-Sheng reactor due to axion coupling to photon or electron, respectively. The search places model-independent limits on the products $G_{A\gamma\gamma} G_{ANN}$ and $G_{Aee} G_{ANN}$ for $m(A^0)$ less than the MeV range.			
85 ALTMANN 95 looked for A^0 decaying into e^+e^- from the Bugey5 nuclear reactor. They obtain an upper limit on the A^0 production rate of $\omega(A^0)/\omega(\gamma) \times \text{B}(A^0 \rightarrow e^+e^-) < 10^{-16}$ for $m_{A^0} = 1.5$ MeV at 90% CL. The limit is weaker for heavier A^0 . In the case of a standard axion, this limit excludes a mass in the range $2m_e < m_{A^0} < 4.8$ MeV at 90% CL. See Fig. 5 of their paper for exclusion limits of axion-like resonances Z^0 in the (m_{X^0}, f_{X^0}) plane.			
86 KETOV 86 searched for A^0 at the Rovno nuclear power plant. They found an upper limit on the A^0 production probability of $0.8 [100 \text{ keV}/m_{A^0}]^6 \times 10^{-6}$ per fission. In the standard axion model, this corresponds to $m_{A^0} > 150$ keV. Not valid for $m_{A^0} \gtrsim 1$ MeV.			
87 KOCH 86 searched for $A^0 \rightarrow \gamma\gamma$ at nuclear power reactor Biblis A. They found an upper limit on the A^0 production rate of $\omega(A^0)/\omega(\gamma(M1)) < 1.5 \times 10^{-10}$ (CL=95%). Standard axion with $m_{A^0} = 250$ keV gives 10^{-5} for the ratio. Not valid for $m_{A^0} > 1022$ keV.			
88 DATAR 82 looked for $A^0 \rightarrow 2\gamma$ in neutron capture ($np \rightarrow dA^0$) at Tarapur 500 MW reactor. Sensitive to sum of $l = 0$ and $l = 1$ amplitudes. With ZEHNDER 81 [$l = 0$ - ($l = 1$)] result, assert nonexistence of standard A^0 .			
89 VUILLEUMIER 81 is at Grenoble reactor. Set limit $m_{A^0} < 280$ keV.			

A^0 (Axion) and Other Light Boson (X^0) Searches in Nuclear Transitions

Limits are for branching ratio.

VALUE	CL%	DOCUMENT ID	TECN	COMMENT
• • • We do not use the following data for averages, fits, limits, etc. • • •				
$< 8.5 \times 10^{-6}$	90	90 DERBIN 02	CNTR	^{125}mTe decay
		91 DEBOER 97c	RVUE	M1 transitions
$< 5.5 \times 10^{-10}$	95	92 TSUNODA 95	CNTR	^{252}Cf fission, $A^0 \rightarrow ee$
$< 1.2 \times 10^{-6}$	95	93 MINOWA 93	CNTR	$^{139}\text{La}^* \rightarrow ^{139}\text{La}A^0$
$< 2 \times 10^{-4}$	90	94 HICKS 92	CNTR	^{35}S decay, $A^0 \rightarrow \gamma\gamma$
$< 1.5 \times 10^{-9}$	95	95 ASANUMA 90	CNTR	^{241}Am decay
$< (0.4-10) \times 10^{-3}$	95	96 DEBOER 90	CNTR	$^8\text{Be}^* \rightarrow ^8\text{Be}A^0$ $A^0 \rightarrow e^+e^-$
$< (0.2-1) \times 10^{-3}$	90	97 BINI 89	CNTR	$^{16}\text{O}^* \rightarrow ^{16}\text{O}X^0$ $X^0 \rightarrow e^+e^-$
		98 AVIGNONE 88	CNTR	$\text{Cu}^* \rightarrow \text{Cu}A^0$ ($A^0 \rightarrow 2\gamma$, $A^0 e \rightarrow \gamma e$, $A^0 Z \rightarrow \gamma Z$)
$< 1.5 \times 10^{-4}$	90	99 DATAR 88	CNTR	$^{12}\text{C}^* \rightarrow ^{12}\text{C}A^0$ $A^0 \rightarrow e^+e^-$
$< 5 \times 10^{-3}$	90	100 DEBOER 88c	CNTR	$^{16}\text{O}^* \rightarrow ^{16}\text{O}X^0$ $X^0 \rightarrow e^+e^-$
$< 3.4 \times 10^{-5}$	95	101 DOEHNER 88	SPEC	$^2\text{H}^*, A^0 \rightarrow e^+e^-$
$< 4 \times 10^{-4}$	95	102 SAVAGE 88	CNTR	Nuclear decay (isovector)

See key on page 405

Gauge & Higgs Boson Particle Listings

Axions (A^0) and Other Very Light Bosons

< 3 × 10 ⁻³	95	102 SAVAGE	88 CNTR	Nuclear decay (isoscalar)
<10.6 × 10 ⁻²	90	103 HALLIN	86 SPEC	⁶ Li isovector decay
<10.8	90	103 HALLIN	86 SPEC	¹⁰ B isoscalar decays
< 2.2	90	103 HALLIN	86 SPEC	¹⁴ N isoscalar decays
< 4 × 10 ⁻⁴	90	104 SAVAGE	86B CNTR	¹⁴ N*
		105 ANANEV	85 CNTR	Li*, deut* A ⁰ → 2γ
		106 CAVAGNAC	83 CNTR	⁹⁷ Nb*, deut* transition A ⁰ → 2γ
		107 ALEKSEEV	82B CNTR	Li*, deut* transition A ⁰ → 2γ
		108 LEHMANN	82 CNTR	Cu* → CuA ⁰ (A ⁰ → 2γ)
		109 ZEHNDER	82 CNTR	Li*, Nb* decay, n-capt.
		110 ZEHNDER	81 CNTR	Ba* → BaA ⁰ (A ⁰ → 2γ)
		111 CALAPRICE	79	Carbon

none 4 × 10 ⁻¹⁶ –4.5 × 10 ⁻¹²	90	112 BROSS	91 BDMP	$eN \rightarrow eA^0N$ ($A^0 \rightarrow ee$)
		113 GUO	90 BDMP	$eN \rightarrow eA^0N$ ($A^0 \rightarrow ee$)
		114 BJORKEN	88 CALO	$A \rightarrow e^+e^-$ or 2γ
		115 BLINOV	88 MD1	$ee \rightarrow eeA^0$ ($A^0 \rightarrow ee$)
none 1 × 10 ⁻¹⁴ –1 × 10 ⁻¹⁰	90	116 RIORDAN	87 BDMP	$eN \rightarrow eA^0N$ ($A^0 \rightarrow ee$)
none 1 × 10 ⁻¹⁴ –1 × 10 ⁻¹¹	90	117 BROWN	86 BDMP	$eN \rightarrow eA^0N$ ($A^0 \rightarrow ee$)
none 6 × 10 ⁻¹⁴ –9 × 10 ⁻¹¹	95	118 DAVIER	86 BDMP	$eN \rightarrow eA^0N$ ($A^0 \rightarrow ee$)
none 3 × 10 ⁻¹³ –1 × 10 ⁻⁷	90	119 KONAKA	86 BDMP	$eN \rightarrow eA^0N$ ($A^0 \rightarrow ee$)

- ⁹⁰ DERBIN 02 looked for the axion emission in an M1 transition in ¹²⁵Te decay. They looked for a possible presence of a shifted energy spectrum in gamma rays due to the undetected axion.
- ⁹¹ DEBOER 97C reanalyzed the existent data on Nuclear M1 transitions and find that a 9 MeV boson decaying into e^+e^- would explain the excess of events with large opening angles. See also DEBOER 01 for follow-up experiments.
- ⁹² TSUNODA 95 looked for axion emission when ²⁵²Cf undergoes a spontaneous fission, with the axion decaying into e^+e^- . The bound is for $m_{A^0}=40$ MeV. It improves to 2.5×10^{-5} for $m_{A^0}=200$ MeV.
- ⁹³ MINOWA 93 studied chain process, ¹³⁹Ce → ¹³⁹La* by electron capture and M1 transition of ¹³⁹La* to the ground state. It does not assume decay modes of A^0 . The bound applies for $m_{A^0} < 166$ keV.
- ⁹⁴ HICKS 92 bound is applicable for $\tau_{X^0} < 4 \times 10^{-11}$ sec.
- ⁹⁵ The ASANUMA 90 limit is for the branching fraction of X^0 emission per ²⁴¹Am α decay and valid for $\tau_{X^0} < 3 \times 10^{-11}$ s.
- ⁹⁶ The DEBOER 90 limit is for the branching ratio ⁸Be* (18.15 MeV, 1⁺) → ⁸BeA⁰, $A^0 \rightarrow e^+e^-$ for the mass range $m_{A^0} = 4-15$ MeV.
- ⁹⁷ The BINI 89 limit is for the branching fraction of ¹⁶O*(6.05 MeV, 0⁺) → ¹⁶OX⁰, $X^0 \rightarrow e^+e^-$ for $m_{X^0} = 1.5-3.1$ MeV. $\tau_{X^0} \lesssim 10^{-11}$ s is assumed. The spin-parity of X is restricted to 0⁺ or 1⁻.
- ⁹⁸ AVIGNONE 88 looked for the 1115 keV transition $C^* \rightarrow CuA^0$, either from $A^0 \rightarrow 2\gamma$ in-flight decay or from the secondary A^0 interactions by Compton and by Primakoff processes. Limits for axion parameters are obtained for $m_{A^0} < 1.1$ MeV.
- ⁹⁹ DATAR 88 rule out light pseudoscalar particle emission through its decay $A^0 \rightarrow e^+e^-$ in the mass range 1.02–2.5 MeV and lifetime range 10^{-13} – 10^{-8} s. The above limit is for $\tau = 5 \times 10^{-13}$ s and $m = 1.7$ MeV; see the paper for the τ -m dependence of the limit.
- ¹⁰⁰ The limit is for the branching fraction of ¹⁶O*(6.05 MeV, 0⁺) → ¹⁶OX⁰, $X^0 \rightarrow e^+e^-$ against internal pair conversion for $m_{X^0} = 1.7$ MeV and $\tau_{X^0} < 10^{-11}$ s. Similar limits are obtained for $m_{X^0} = 1.3-3.2$ MeV. The spin parity of X^0 must be either 0⁺ or 1⁻. The limit at 1.7 MeV is translated into a limit for the X^0 -nucleon coupling constant: $g_{X^0 N N}^2/4\pi < 2.3 \times 10^{-9}$.
- ¹⁰¹ The DOEHNER 88 limit is for $m_{A^0} = 1.7$ MeV, $\tau(A^0) < 10^{-10}$ s. Limits less than 10^{-4} are obtained for $m_{A^0} = 1.2-2.2$ MeV.
- ¹⁰² SAVAGE 88 looked for A^0 that decays into e^+e^- in the decay of the 9.17 MeV $J^P = 2^+$ state in ¹⁴N, 17.64 MeV state $J^P = 1^+$ in ⁸Be, and the 18.15 MeV state $J^P = 1^+$ in ⁸Be. This experiment constrains the isovector coupling of A^0 to hadrons, if $m_{A^0} = (1.1 \rightarrow 2.2)$ MeV and the isoscalar coupling of A^0 to hadrons, if $m_{A^0} = (1.1 \rightarrow 2.6)$ MeV. Both limits are valid only if $\tau(A^0) \lesssim 1 \times 10^{-11}$ s.
- ¹⁰³ Limits are for $\Gamma(A^0(1.8 \text{ MeV}))/\Gamma(\pi M1)$; i.e., for 1.8 MeV axion emission normalized to the rate for internal emission of e^+e^- pairs. Valid for $\tau_{A^0} < 2 \times 10^{-11}$ s. ⁶Li isovector decay data strongly disfavor PECCEI 86 model I, whereas the ¹⁰B and ¹⁴N isoscalar decay data strongly reject PECCEI 86 model II and III.
- ¹⁰⁴ SAVAGE 86B looked for A^0 that decays into e^+e^- in the decay of the 9.17 MeV $J^P = 2^+$ state in ¹⁴N. Limit on the branching fraction is valid if $\tau_{A^0} \lesssim 1 \times 10^{-11}$ s for $m_{A^0} = (1.1-1.7)$ MeV. This experiment constrains the iso-vector coupling of A^0 to hadrons.
- ¹⁰⁵ ANANEV 85 with IBR-2 pulsed reactor exclude standard A^0 at CL = 95% masses below 470 keV (Li* decay) and below $2m_d$ for deuteron* decay.
- ¹⁰⁶ CAVAGNAC 83 at Bugey reactor exclude axion at any ⁹⁷Nb* decay and axion with m_{A^0} between 275 and 288 keV (deuteron* decay).
- ¹⁰⁷ ALEKSEEV 82 with IBR-2 pulsed reactor exclude standard A^0 at CL = 95% mass-ranges $m_{A^0} < 400$ keV (Li* decay) and $330 \text{ keV} < m_{A^0} < 2.2$ MeV. (deuteron* decay).
- ¹⁰⁸ LEHMANN 82 obtained $A^0 \rightarrow 2\gamma$ rate $< 6.2 \times 10^{-5}/s$ (CL = 95%) excluding m_{A^0} between 100 and 1000 keV.
- ¹⁰⁹ ZEHNDER 82 used Gosgen 2.8GW light-water reactor to check A^0 production. No 2γ peak in Li*, Nb* decay (both single p transition) nor in n capture (combined with previous Ba* negative result) rules out standard A^0 . Set limit $m_{A^0} < 60$ keV for any A^0 .
- ¹¹⁰ ZEHNDER 81 looked for Ba* → A^0 Ba transition with $A^0 \rightarrow 2\gamma$. Obtained 2γ coincidence rate $< 2.2 \times 10^{-5}/s$ (CL = 95%) excluding $m_{A^0} > 160$ keV (or 200 keV depending on Higgs mixing). However, see BARROSO 81.
- ¹¹¹ CALAPRICE 79 saw no axion emission from excited states of carbon. Sensitive to axion mass between 1 and 15 MeV.

- ¹¹² The listed BROSS 91 limit is for $m_{A^0} = 1.14$ MeV. $B(A^0 \rightarrow e^+e^-) = 1$ assumed. Excluded domain in the $\tau_{A^0}-m_{A^0}$ plane extends up to $m_{A^0} \approx 7$ MeV (see Fig. 5). Combining with electron $g-2$ constraint, axions coupling only to e^+e^- ruled out for $m_{A^0} < 4.8$ MeV (90% CL).
- ¹¹³ GUO 90 use the same apparatus as BROWN 86 and improve the previous limit in the shorter lifetime region. Combined with $g-2$ constraint, axions coupling only to e^+e^- are ruled out for $m_{A^0} < 2.7$ MeV (90% CL).
- ¹¹⁴ BJORKEN 88 reports limits on axion parameters (f_A, m_A, τ_A) for $m_{A^0} < 200$ MeV from electron beam-dump experiment with production via Primakoff photoproduction, bremsstrahlung from electrons, and resonant annihilation of positrons on atomic electrons.
- ¹¹⁵ BLINOV 88 assume zero spin, $m = 1.8$ MeV and lifetime $< 5 \times 10^{-12}$ s and find $\Gamma(A^0 \rightarrow \gamma\gamma)B(A^0 \rightarrow e^+e^-) < 2$ eV (CL=90%).
- ¹¹⁶ Assumes $A^0\gamma\gamma$ coupling is small and hence Primakoff production is small. Their figure 2 shows limits on axions for $m_{A^0} < 15$ MeV.
- ¹¹⁷ Uses electrons in hadronic showers from an incident 800 GeV proton beam. Limits for $m_{A^0} < 15$ MeV are shown in their figure 3.
- ¹¹⁸ $m_{A^0} = 1.8$ MeV assumed. The excluded domain in the $\tau_{A^0}-m_{A^0}$ plane extends up to $m_{A^0} \approx 14$ MeV, see their figure 4.
- ¹¹⁹ The limits are obtained from their figure 3. Also given is the limit on the $A^0\gamma\gamma-A^0e^+e^-$ coupling plane by assuming Primakoff production.

Search for A^0 (Axion) Resonance in Bhabha Scattering

The limit is for $\Gamma(A^0)[B(A^0 \rightarrow e^+e^-)]^2$.

VALUE (10 ⁻³ eV)	CL%	DOCUMENT ID	TECN	COMMENT
•••	•••	•••	•••	••• We do not use the following data for averages, fits, limits, etc. •••
< 1.3	97	120 HALLIN	92 CNTR	$m_{A^0} = 1.75-1.88$ MeV
none 0.0016-0.47	90	121 HENDERSON	92C CNTR	$m_{A^0} = 1.5-1.86$ MeV
< 2.0	90	122 WU	92 CNTR	$m_{A^0} = 1.56-1.86$ MeV
< 0.013	95	TSERTOS	91 CNTR	$m_{A^0} = 1.832$ MeV
none 0.19-3.3	95	123 WIDMANN	91 CNTR	$m_{A^0} = 1.78-1.92$ MeV
< 5	97	BAUER	90 CNTR	$m_{A^0} = 1.832$ MeV
none 0.09-1.5	95	124 JUDGE	90 CNTR	$m_{A^0} = 1.832$ MeV, elastic
< 1.9	97	125 TSERTOS	89 CNTR	$m_{A^0} = 1.82$ MeV
<(10-40)	97	125 TSERTOS	89 CNTR	$m_{A^0} = 1.51-1.65$ MeV
<(1-2.5)	97	125 TSERTOS	89 CNTR	$m_{A^0} = 1.80-1.86$ MeV
< 31	95	LORENZ	88 CNTR	$m_{A^0} = 1.646$ MeV
< 94	95	LORENZ	88 CNTR	$m_{A^0} = 1.726$ MeV
< 23	95	LORENZ	88 CNTR	$m_{A^0} = 1.782$ MeV
< 19	95	LORENZ	88 CNTR	$m_{A^0} = 1.837$ MeV
< 3.8	97	126 TSERTOS	88 CNTR	$m_{A^0} = 1.832$ MeV
		127 VANKLINKEN	88 CNTR	
		128 MAIER	87 CNTR	
<2500	90	MILLS	87 CNTR	$m_{A^0} = 1.8$ MeV
		129 VONWIMMER	.87 CNTR	

- ¹²⁰ HALLIN 92 quote limits on lifetime, $8 \times 10^{-14} - 5 \times 10^{-13}$ sec depending on mass, assuming $B(A^0 \rightarrow e^+e^-) = 100\%$. They say that TSERTOS 91 overstated their sensitivity by a factor of 3.
- ¹²¹ HENDERSON 92C exclude axion with lifetime $\tau_{A^0} = 1.4 \times 10^{-12} - 4.0 \times 10^{-10}$ s, assuming $B(A^0 \rightarrow e^+e^-) = 100\%$. HENDERSON 92C also exclude a vector boson with $\tau = 1.4 \times 10^{-12} - 6.0 \times 10^{-10}$ s.
- ¹²² WU 92 quote limits on lifetime $> 3.3 \times 10^{-13}$ s assuming $B(A^0 \rightarrow e^+e^-) = 100\%$. They say that TSERTOS 89 overestimate the limit by a factor of $\pi/2$. WU 92 also quote a bound for vector boson, $\tau > 8.2 \times 10^{-13}$ s.
- ¹²³ WIDMANN 91 bound applies exclusively to the case $B(A^0 \rightarrow e^+e^-) = 1$, since the detection efficiency varies substantially as $\Gamma(A^0)_{\text{total}}$ changes. See their Fig. 6.
- ¹²⁴ JUDGE 90 excludes an elastic pseudoscalar e^+e^- resonance for 4.5×10^{-13} s $< \tau(A^0) < 7.5 \times 10^{-12}$ s (95% CL) at $m_{A^0} = 1.832$ MeV. Comparable limits can be set for $m_{A^0} = 1.776-1.856$ MeV.
- ¹²⁵ See also TSERTOS 88B in references.
- ¹²⁶ The upper limit listed in TSERTOS 88 is too large by a factor of 4. See TSERTOS 88B, footnote 3.
- ¹²⁷ VANKLINKEN 88 looked for relatively long-lived resonance ($\tau = 10^{-10}-10^{-12}$ s). The sensitivity is not sufficient to exclude such a narrow resonance.
- ¹²⁸ MAIER 87 obtained limits $R\Gamma \lesssim 60$ eV (100 eV) at $m_{A^0} \approx 1.64$ MeV (1.83 MeV) for energy resolution $\Delta E_{\text{cm}} \approx 3$ keV, where R is the resonance cross section normalized

A^0 (Axion) Limits from Its Electron Coupling

Limits are for $\tau(A^0 \rightarrow e^+e^-)$.

VALUE (s)	CL%	DOCUMENT ID	TECN	COMMENT
-----------	-----	-------------	------	---------

••• We do not use the following data for averages, fits, limits, etc. •••

Gauge & Higgs Boson Particle Listings

Axions (A^0) and Other Very Light Bosons

to that of Bhabha scattering, and $\Gamma = \Gamma_{e^+e^-}^2/\Gamma_{\text{total}}$. For a discussion implying that $\Delta E_{\text{cm}} \simeq 10$ keV, see TSERTOS 89.

129 VONWIMMERSPERG 87 measured Bhabha scattering for $E_{\text{cm}} = 1.37\text{--}1.86$ MeV and found a possible peak at 1.73 with $\int \sigma dE_{\text{cm}} = 14.5 \pm 6.8$ keV-b. For a comment and a reply, see VANKLINKEN 88B and VONWIMMERSPERG 88. Also see CONNELL 88.

Search for A^0 (Axion) Resonance in $e^+e^- \rightarrow \gamma\gamma$

The limit is for $\Gamma(A^0 \rightarrow e^+e^-)\Gamma(A^0 \rightarrow \gamma\gamma)/\Gamma_{\text{total}}$

VALUE (10^{-3} eV)	CL%	DOCUMENT ID	TECN	COMMENT
••• We do not use the following data for averages, fits, limits, etc. •••				
< 0.18	95	VO	94 CNTR	$m_{A^0} = 1.1$ MeV
< 1.5	95	VO	94 CNTR	$m_{A^0} = 1.4$ MeV
< 12	95	VO	94 CNTR	$m_{A^0} = 1.7$ MeV
< 6.6	95	130 TRZASKA	91 CNTR	$m_{A^0} = 1.8$ MeV
< 4.4	95	WIDMANN	91 CNTR	$m_{A^0} = 1.78\text{--}1.92$ MeV
		131 FOX	89 CNTR	
< 0.11	95	132 MINOWA	89 CNTR	$m_{A^0} = 1.062$ MeV
< 33	97	CONNELL	88 CNTR	$m_{A^0} = 1.580$ MeV
< 42	97	CONNELL	88 CNTR	$m_{A^0} = 1.642$ MeV
< 73	97	CONNELL	88 CNTR	$m_{A^0} = 1.782$ MeV
< 79	97	CONNELL	88 CNTR	$m_{A^0} = 1.832$ MeV

130 TRZASKA 91 also give limits in the range $(6.6\text{--}30) \times 10^{-3}$ eV (95%CL) for $m_{A^0} = 1.6\text{--}2.0$ MeV.

131 FOX 89 measured positron annihilation with an electron in the source material into two photons and found no signal at 1.062 MeV ($< 9 \times 10^{-5}$ of two-photon annihilation at rest).

132 Similar limits are obtained for $m_{A^0} = 1.045\text{--}1.085$ MeV.

Search for X^0 (Light Boson) Resonance in $e^+e^- \rightarrow \gamma\gamma\gamma$

The limit is for $\Gamma(X^0 \rightarrow e^+e^-)\Gamma(X^0 \rightarrow \gamma\gamma\gamma)/\Gamma_{\text{total}}$. C invariance forbids spin-0 X^0 coupling to both e^+e^- and $\gamma\gamma\gamma$.

VALUE (10^{-3} eV)	CL%	DOCUMENT ID	TECN	COMMENT
••• We do not use the following data for averages, fits, limits, etc. •••				
< 0.2	95	133 VO	94 CNTR	$m_{X^0} = 1.1\text{--}1.9$ MeV
< 1.0	95	134 VO	94 CNTR	$m_{X^0} = 1.1$ MeV
< 2.5	95	134 VO	94 CNTR	$m_{X^0} = 1.4$ MeV
< 120	95	134 VO	94 CNTR	$m_{X^0} = 1.7$ MeV
< 3.8	95	135 SKALSEY	92 CNTR	$m_{X^0} = 1.5$ MeV

133 VO 94 looked for $X^0 \rightarrow \gamma\gamma\gamma$ decaying at rest. The precise limits depend on m_{X^0} . See Fig. 2(b) in paper.

134 VO 94 looked for $X^0 \rightarrow \gamma\gamma\gamma$ decaying in flight.

135 SKALSEY 92 also give limits 4.3 for $m_{X^0} = 1.54$ and 7.5 for 1.64 MeV. The spin of X^0 is assumed to be one.

Light Boson (X^0) Search in Nonresonant e^+e^- Annihilation at Rest

Limits are for the ratio of $n\gamma + X^0$ production relative to $\gamma\gamma$.

VALUE (units 10^{-6})	CL%	DOCUMENT ID	TECN	COMMENT
••• We do not use the following data for averages, fits, limits, etc. •••				
< 4.2	90	136 MITSUI	96 CNTR	γX^0
< 4	68	SKALSEY	95 CNTR	γX^0
< 40	68	SKALSEY	95 RVUE	γX^0
< 0.18	90	139 ADACHI	94 CNTR	$\gamma\gamma X^0, X^0 \rightarrow \gamma\gamma$
< 0.26	90	140 ADACHI	94 CNTR	$\gamma\gamma X^0, X^0 \rightarrow \gamma\gamma$
< 0.33	90	141 ADACHI	94 CNTR	$\gamma X^0, X^0 \rightarrow \gamma\gamma\gamma$

136 MITSUI 96 looked for a monochromatic γ . The bound applies for a vector X^0 with $C = -1$ and $m_{X^0} < 200$ keV. They derive an upper bound on eeX^0 coupling and hence on the branching ratio $B(\alpha\text{-Ps} \rightarrow \gamma\gamma X^0) < 6.2 \times 10^{-6}$. The bounds weaken for heavier X^0 .

137 SKALSEY 95 looked for a monochromatic γ without an accompanying γ in e^+e^- annihilation. The bound applies for scalar and vector X^0 with $C = -1$ and $m_{X^0} = 100\text{--}1000$ keV.

138 SKALSEY 95 reinterpreted the bound on γA^0 decay of $\alpha\text{-Ps}$ by ASAI 91 where 3% of delayed annihilations are not from 3S_1 states. The bound applies for scalar and vector X^0 with $C = -1$ and $m_{X^0} = 0\text{--}800$ keV.

139 ADACHI 94 looked for a peak in the $\gamma\gamma$ invariant mass distribution in $\gamma\gamma\gamma\gamma$ production from e^+e^- annihilation. The bound applies for $m_{X^0} = 70\text{--}800$ keV.

140 ADACHI 94 looked for a peak in the missing-mass mass distribution in $\gamma\gamma$ channel, using $\gamma\gamma\gamma$ production from e^+e^- annihilation. The bound applies for $m_{X^0} < 800$ keV.

141 ADACHI 94 looked for a peak in the missing mass distribution in $\gamma\gamma\gamma$ channel, using $\gamma\gamma\gamma\gamma$ production from e^+e^- annihilation. The bound applies for $m_{X^0} = 200\text{--}900$ keV.

Searches for Goldstone Bosons (X^0)

(Including Horizontal Bosons and Majorons.) Limits are for branching ratios.

VALUE	CL%	DOCUMENT ID	TECN	COMMENT
••• We do not use the following data for averages, fits, limits, etc. •••				

142	LESSA	07	RVUE	Meson, ℓ decays to Majoron
143	DIAZ	98	THEO	$H^0 \rightarrow X^0 X^0, A^0 \rightarrow X^0 X^0 X^0$, Majoron
144	BOBRAKOV	91		Electron quasi-magnetic interaction
< 3.3×10^{-2}	95	145 ALBRECHT	90E ARG	$\tau \rightarrow \mu X^0$. Familon
< 1.8×10^{-2}	95	145 ALBRECHT	90E ARG	$\tau \rightarrow e X^0$. Familon
< 6.4×10^{-9}	90	146 ATIYA	90 B787	$K^+ \rightarrow \pi^+ X^0$. Familon
< 1.1×10^{-9}	90	147 BOLTON	88 CBOX	$\mu^+ \rightarrow e^+ \gamma X^0$. Familon
		148 CHANDA	88 ASTR	Sun, Majoron
		149 CHOI	88 ASTR	Majoron, SN 1987A
< 5×10^{-6}	90	150 PICCIOTTO	88 CNTR	$\pi \rightarrow e\nu X^0$, Majoron
< 1.3×10^{-9}	90	151 GOLDMAN	87 CNTR	$\mu \rightarrow e\gamma X^0$. Familon
< 3×10^{-4}	90	152 BRYMAN	86B RVUE	$\mu \rightarrow e X^0$. Familon
< 1×10^{-10}	90	153 EICHLER	86 SPEC	$\mu^+ \rightarrow e^+ X^0$. Familon
< 2.6×10^{-6}	90	154 JODIDIO	86 SPEC	$\mu^+ \rightarrow e^+ X^0$. Familon
		155 BALTRUSAITIS..85	MRK3	$\tau \rightarrow \ell X^0$. Familon
		156 DICUS	83 COSM	$\nu(\text{hvy}) \rightarrow \nu(\text{light}) X^0$

142 LESSA 07 consider decays of the form Meson $\rightarrow \ell\nu$ Majoron and $\ell \rightarrow \ell'\nu\overline{\nu}$ Majoron and use existing data to derive limits on the neutrino-Majoron Yukawa couplings $g_{\alpha\beta}$ ($\alpha, \beta = e, \mu, \tau$). Their best limits are $|g_{e\alpha}|^2 < 5.5 \times 10^{-6}$, $|g_{\mu\alpha}|^2 < 4.5 \times 10^{-5}$, $|g_{\tau\alpha}|^2 < 5.5 \times 10^{-2}$ at CL = 90%.

143 DIAZ 98 studied models of spontaneously broken lepton number with both singlet and triplet Higgses. They obtain limits on the parameter space from invisible decay $Z \rightarrow H^0 A^0 \rightarrow X^0 X^0 X^0 X^0$ and $e^+e^- \rightarrow Z H^0$ with $H^0 \rightarrow X^0 X^0$.

144 BOBRAKOV 91 searched for anomalous magnetic interactions between polarized electrons expected from the exchange of a massless pseudoscalar boson (arion). A limit $x_e^2 < 2 \times 10^{-4}$ (95%CL) is found for the effective anomalous magneton parametrized as $x_e(G_F/8\pi\sqrt{2})^{1/2}$.

145 ALBRECHT 90E limits are for $B(\tau \rightarrow \ell X^0)/B(\tau \rightarrow \ell\nu\overline{\nu})$. Valid for $m_{X^0} < 100$ MeV. The limits rise to 7.1% (for μ), 5.0% (for e) for $m_{X^0} = 500$ MeV.

146 ATIYA 90 limit is for $m_{X^0} = 0$. The limit $B < 1 \times 10^{-8}$ holds for $m_{X^0} < 95$ MeV. For the reduction of the limit due to finite lifetime of X^0 , see their Fig. 3.

147 BOLTON 88 limit corresponds to $F > 3.1 \times 10^9$ GeV, which does not depend on the chirality property of the coupling.

148 CHANDA 88 find $v_T < 10$ MeV for the weak-triplet Higgs vacuum expectation value in Gelmini-Roncadelli model, and $v_S > 5.8 \times 10^6$ GeV in the singlet Majoron model.

149 CHOI 88 used the observed neutrino flux from the supernova SN1987A to exclude the neutrino Majoron Yukawa coupling h in the range $2 \times 10^{-5} < h < 3 \times 10^{-4}$ for the interaction $L_{\text{int}} = \frac{1}{2} i h \overline{\psi}_\nu \gamma_5 \psi_\nu \phi_X$. For several families of neutrinos, the limit applies for $(\Sigma h_i^2)^{1/4}$.

150 PICCIOTTO 88 limit applies when $m_{X^0} < 55$ MeV and $\tau_{X^0} > 2$ ns, and it decreases to 4×10^{-7} at $m_{X^0} = 125$ MeV, beyond which no limit is obtained.

151 GOLDMAN 87 limit corresponds to $F > 2.9 \times 10^9$ GeV for the family symmetry breaking scale from the Lagrangian $L_{\text{int}} = (1/F) \overline{\psi}_\mu \gamma^{\mu\mu} (a + b\gamma_5) \psi_e \phi_\mu \phi_{X^0}$ with $a^2 + b^2 = 1$.

This is not as sensitive as the limit $F > 9.9 \times 10^9$ GeV derived from the search for $\mu^+ \rightarrow e^+ X^0$ by JODIDIO 86, but does not depend on the chirality property of the coupling.

152 Limits are for $\Gamma(\mu \rightarrow e X^0)/\Gamma(\mu \rightarrow e\nu\overline{\nu})$. Valid when $m_{X^0} = 0\text{--}93.4, 98.1\text{--}103.5$ MeV.

153 EICHLER 86 looked for $\mu^+ \rightarrow e^+ X^0$ followed by $X^0 \rightarrow e^+e^-$. Limits on the branching fraction depend on the mass and lifetime of X^0 . The quoted limits are valid when $\tau_{X^0} \lesssim 3 \times 10^{-10}$ s if the decays are kinematically allowed.

154 JODIDIO 86 corresponds to $F > 9.9 \times 10^9$ GeV for the family symmetry breaking scale with the parity-conserving effective Lagrangian $L_{\text{int}} = (1/F) \overline{\psi}_\mu \gamma^{\mu\mu} \psi_e \phi_\mu \phi_{X^0}$.

155 BALTRUSAITIS 85 search for light Goldstone boson (X^0) of broken U(1). CL = 95% limits are $B(\tau \rightarrow \mu^+ X^0)/B(\tau \rightarrow \mu^+ \nu\nu) < 0.125$ and $B(\tau \rightarrow e^+ X^0)/B(\tau \rightarrow e^+ \nu\nu) < 0.04$. Inferred limit for the symmetry breaking scale is $m > 3000$ TeV.

156 The primordial heavy neutrino must decay into ν and familon, f_A , early so that the red-shifted decay products are below critical density, see their table. In addition, $K \rightarrow \pi f_A$ and $\mu \rightarrow e f_A$ are unseen. Combining these excludes $m_{\text{heavy}\nu}$ between 5×10^{-5} and 5×10^{-4} MeV (μ decay) and $m_{\text{heavy}\nu}$ between 5×10^{-5} and 0.1 MeV (K -decay).

Majoron Searches in Neutrinoless Double β Decay

Limits are for the half-life of neutrinoless $\beta\beta$ decay with a Majoron emission.

No experiment currently claims any such evidence. Only the best or comparable limits for each isotope are reported. Also see the reviews ZUBER 98 and FAESSLER 98B.

$t_{1/2} (10^{21}$ yr)	CL%	ISOTOPE	TRANSITION	METHOD	DOCUMENT ID
> 7200	90	128Te	CNTR		157 BERNATOW... 92
••• We do not use the following data for averages, fits, limits, etc. •••					
> 1.52	90	150Nd	$0\nu 1\chi$	NEMO-3	158 ARGYRIADES 09
> 27	90	100Mo	$0\nu 1\chi$	NEMO-3	159 ARNOLD 06
> 15	90	82Se	$0\nu 1\chi$	NEMO-3	160 ARNOLD 06
> 14	90	100Mo	$0\nu 1\chi$	NEMO-3	161 ARNOLD 04
> 12	90	82Se	$0\nu 1\chi$	NEMO-3	162 ARNOLD 04
> 2.2	90	130Te	$0\nu 1\chi$	Cryog. det.	163 ARNABOLDI 03
> 0.9	90	130Te	$0\nu 2\chi$	Cryog. det.	164 ARNABOLDI 03
> 8	90	116Cd	$0\nu 1\chi$	CdWO ₄ scint.	165 DANEVICH 03
> 0.8	90	116Cd	$0\nu 2\chi$	CdWO ₄ scint.	166 DANEVICH 03
> 500	90	136Xe	$0\nu \chi$	Liquid Xe Scint.	167 BERNABEI 02b
> 5.8	90	100Mo	$0\nu \chi$	ELEGANT V	168 FUSHIMI 02
> 0.32	90	100Mo	$0\nu \chi$	Liq. Ar ioniz.	169 ASHITKOV 01

See key on page 405

Gauge & Higgs Boson Particle Listings

Axions (A^0) and Other Very Light Bosons

> 0.0035 90 ¹⁶⁰Gd $0\nu\chi$ ¹⁶⁰Gd₂SiO₅:Ce ¹⁷⁰DANEVICH 01
 > 0.013 90 ¹⁶⁰Gd $0\nu2\chi$ ¹⁶⁰Gd₂SiO₅:Ce ¹⁷¹DANEVICH 01
 > 2.3 90 ⁸²Se $0\nu\chi$ NEMO 2 ¹⁷²ARNOLD 00
 > 0.31 90 ⁹⁶Zr $0\nu\chi$ NEMO 2 ¹⁷³ARNOLD 00
 > 0.63 90 ⁸²Se $0\nu2\chi$ NEMO 2 ¹⁷⁴ARNOLD 00
 > 0.063 90 ⁹⁶Zr $0\nu2\chi$ NEMO 2 ¹⁷⁴ARNOLD 00
 > 0.16 90 ¹⁰⁰Mo $0\nu2\chi$ NEMO 2 ¹⁷⁴ARNOLD 00
 > 2.4 90 ⁸²Se $0\nu\chi$ NEMO 2 ¹⁷⁵ARNOLD 98
 > 7.2 90 ¹³⁶Xe $0\nu2\chi$ TPC ¹⁷⁶LUESCHER 98
 > 7.91 90 ⁷⁶Ge SPEC ¹⁷⁷GUENTHER 96
 > 17 90 ⁷⁶Ge CNTR BECK 93

¹⁵⁷BERNATOWICZ 92 studied double- β decays of ¹²⁸Te and ¹³⁰Te, and found the ratio $\tau(^{130}\text{Te})/\tau(^{128}\text{Te}) = (3.52 \pm 0.11) \times 10^{-4}$ in agreement with relatively stable theoretical predictions. The bound is based on the requirement that Majoron-emitting decay cannot be larger than the observed double-beta rate of ¹²⁸Te of $(7.7 \pm 0.4) \times 10^{24}$ year. We calculated 90% CL limit as $(7.7-1.28 \times 0.4=7.2) \times 10^{24}$.

¹⁵⁸ARGYRIADES 09 use ¹⁵⁰Nd data taken with the NEMO-3 tracking detector. The reported limit corresponds to $\langle g_{\nu\chi} \rangle < 1.7-3.0 \times 10^{-4}$ using a range of nuclear matrix elements that include the effect of nuclear deformation.

¹⁵⁹ARNOLD 06 use ¹⁰⁰Mo data taken with the NEMO-3 tracking detector. The reported limit corresponds to $\langle g_{\nu\chi} \rangle < (0.4-1.8) \times 10^{-4}$ using a range of matrix element calculations. Supersedes ARNOLD 04.

¹⁶⁰NEMO-3 tracking calorimeter is used in ARNOLD 06. Reported half-life limit for ⁸²Se corresponds to $\langle g_{\nu\chi} \rangle < (0.66-1.9) \times 10^{-4}$ using a range of matrix element calculations. Supersedes ARNOLD 04.

¹⁶¹ARNOLD 04 use the NEMO-3 tracking detector. The limit corresponds to $\langle g_{\nu\chi} \rangle < (0.5-0.9)10^{-4}$ using the matrix elements of SIMKOVIĆ 99, STOICA 01 and CIVITARESE 03.

¹⁶²ARNOLD 04 use the NEMO-3 tracking detector. The limit corresponds to $\langle g_{\nu\chi} \rangle < (0.7-1.6)10^{-4}$ using the matrix elements of SIMKOVIĆ 99, STOICA 01 and CIVITARESE 03.

¹⁶³Supersedes ALESSANDRELLO 00. Array of TeO₂ crystals in high resolution cryogenic calorimeter. Some enriched in ¹³⁰Te. Derive $\langle g_{\nu\chi} \rangle < 17-33 \times 10^{-5}$ depending on matrix element.

¹⁶⁴Supersedes ALESSANDRELLO 00. Cryogenic calorimeter search.

¹⁶⁵Limit for the $0\nu\chi$ decay with Majoron emission of ¹¹⁶Cd using enriched CdWO₄ scintillators. $\langle g_{\nu\chi} \rangle < 4.6-8.1 \times 10^{-5}$ depending on the matrix element. Supersedes DANEVICH 00.

¹⁶⁶Limit for the $0\nu2\chi$ decay of ¹¹⁶Cd. Supersedes DANEVICH 00.

¹⁶⁷BERNABEI 02b obtain limit for $0\nu\chi$ decay with Majoron emission of ¹³⁶Xe using liquid Xe scintillation detector. They derive $\langle g_{\nu\chi} \rangle < 2.0-3.0 \times 10^{-5}$ with several nuclear matrix elements.

¹⁶⁸Replaces TANAKA 93. FUSHIMI 02 derive half-life limit for the $0\nu\chi$ decay by means of tracking calorimeter ELEGANT V. Considering various matrix element calculations, a range of limits for the Majoron-neutrino coupling is given: $\langle g_{\nu\chi} \rangle < (6.3-360) \times 10^{-5}$.

¹⁶⁹ASHITKOV 01 result for $0\nu\chi$ of ¹⁰⁰Mo is less stringent than ARNOLD 00.

¹⁷⁰DANEVICH 01 obtain limit for the $0\nu\chi$ decay with Majoron emission of ¹⁶⁰Gd using Gd₂SiO₅:Ce crystal scintillators.

¹⁷¹DANEVICH 01 obtain limit for the $0\nu2\chi$ decay with 2 Majoron emission of ¹⁶⁰Gd.

¹⁷²ARNOLD 00 reports limit for the $0\nu\chi$ decay with Majoron emission derived from tracking calorimeter NEMO 2. Using ⁸²Se source: $\langle g_{\nu\chi} \rangle < 1.6 \times 10^{-4}$. Matrix element from GUENTHER 96.

¹⁷³Using ⁹⁶Zr source: $\langle g_{\nu\chi} \rangle < 2.6 \times 10^{-4}$. Matrix element from ARNOLD 99.

¹⁷⁴ARNOLD 00 reports limit for the $0\nu2\chi$ decay with two Majoron emission derived from tracking calorimeter NEMO 2.

¹⁷⁵ARNOLD 98 determine the limit for $0\nu\chi$ decay with Majoron emission of ⁸²Se using the NEMO-2 tracking detector. They derive $\langle g_{\nu\chi} \rangle < 2.3-4.3 \times 10^{-4}$ with several nuclear matrix elements.

¹⁷⁶LUESCHER 98 report a limit for the 0ν decay with Majoron emission of ¹³⁶Xe using Xe TPC. This result is more stringent than BARABASH 89. Using the matrix elements of ENGEL 88, they obtain a limit on $\langle g_{\nu\chi} \rangle$ of 2.0×10^{-4} .

¹⁷⁷See Table 1 in GUENTHER 96 for limits on the Majoron coupling in different models.

none 3-8 ¹⁹²BERSHADY 91 ASTR D, K, intergalactic light

< 10 ¹⁹³KIM 91c COSM D, K, mass density of the universe, supersymmetry

< 1 $\times 10^{-3}$ ¹⁹⁴RAFFELT 91B ASTR D,K, SN 1987A

none 10^{-3-3} ¹⁹⁵RESSELL 91 ASTR K, intergalactic light
 BURROWS 90 ASTR D,K, SN 1987A

< 0.02 ¹⁹⁶ENGEL 90 ASTR D,K, SN 1987A

< 1 $\times 10^{-3}$ ¹⁹⁷RAFFELT 90D ASTR D, red giant

<(1.4-10) $\times 10^{-3}$ ¹⁹⁸BURROWS 89 ASTR D,K, SN 1987A

< 3.6 $\times 10^{-4}$ ¹⁹⁹ERICSON 89 ASTR D,K, SN 1987A

< 12 ²⁰⁰MAYLE 89 ASTR D,K, SN 1987A
 CHANDA 88 ASTR D, Sun
 RAFFELT 88 ASTR D,K, SN 1987A

< 0.07 ²⁰¹RAFFELT 88B ASTR red giant
 FRIEMAN 87 ASTR D, red giant

< 0.7 ²⁰²RAFFELT 87 ASTR K, red giant

< 2-5 ²⁰³TURNER 87 COSM K, thermal production

< 0.01 ²⁰³DEARBORN 86 ASTR D, red giant

< 0.6 ²⁰³RAFFELT 86 ASTR D, red giant

< 0.7 ²⁰⁴RAFFELT 86 ASTR K, red giant

< 0.03 ²⁰⁴RAFFELT 86B ASTR D, white dwarf

< 1 ²⁰⁵KAPLAN 85 ASTR K, red giant

< 0.003-0.02 ²⁰⁵IWAMOTO 84 ASTR D, K, neutron star

> 1 $\times 10^{-5}$ ²⁰⁶ABBOTT 83 COSM D,K, mass density of the universe

> 1 $\times 10^{-5}$ ²⁰⁶DINE 83 COSM D,K, mass density of the universe

< 0.04 ²⁰⁶ELLIS 83B ASTR D, red giant

> 1 $\times 10^{-5}$ ²⁰⁶PRESKILL 83 COSM D,K, mass density of the universe

< 0.1 ²⁰⁶BARROSO 82 ASTR D, red giant

< 1 ²⁰⁶FUKUGITA 82 ASTR D, stellar cooling

< 0.07 ²⁰⁶FUKUGITA 82B ASTR D, red giant

¹⁷⁸ANDRIAMONJE 09 look for solar axions produced from the thermally excited 14.4 keV level of ⁵⁷Fe. They show limits on the axion-nucleon \times axion-photon coupling assuming $m_A < 0.03$ eV.

¹⁷⁹DERBIN 09A look for Primakoff-produced solar axions in the resonant excitation of ¹⁶⁹Tm, constraining the axion-photon \times axion-nucleon couplings.

¹⁸⁰KEKEZ 09 look at axio-electric effect of solar axions in HPGe detectors. The one-loop axion-electron coupling for hadronic axions is used.

¹⁸¹This is an update of HANNESTAD 07 including 5 years of WMAP data.

¹⁸²This is an update of HANNESTAD 05a with new cosmological data, notably WMAP (3 years) and baryon acoustic oscillations (BAO). Lyman- α data are left out, in contrast to HANNESTAD 05a and MELCHIORRI 07a, because it is argued that systematic errors are large. It uses Bayesian statistics and marginalizes over a possible neutrino hot dark matter component.

¹⁸³MELCHIORRI 07a is analogous to HANNESTAD 05a, with updated cosmological data, notably WMAP (3 years). Uses Bayesian statistics and marginalizes over a possible neutrino hot dark matter component. Leaving out Lyman- α data, a conservative limit is 1.4 eV.

¹⁸⁴HANNESTAD 05a puts an upper limit on the mass of hadronic axion because in this mass range it would have been thermalized and contribute to the hot dark matter component of the universe. The limit is based on the CMB anisotropy from WMAP, SDSS large scale structure, Lyman α , and the prior Hubble parameter from HST Key Project. A χ^2 statistic is used. Neutrinos are assumed not to contribute to hot dark matter.

¹⁸⁵MORIO 98 points out that a KSVZ axion of this mass range (see CHANG 93) can be a viable hot dark matter of Universe, as long as the model-dependent $g_{A\gamma}$ is accidentally small enough as originally emphasized by KAPLAN 85; see Fig. 1.

¹⁸⁶BORISOV 97 bound is on the axion-electron coupling $g_{ae} < 1 \times 10^{-13}$ from the photo-production of axions off of magnetic fields in the outer layers of neutron stars.

¹⁸⁷KACHELRIESS 97 bound is on the axion-electron coupling $g_{ae} < 1 \times 10^{-10}$ from the production of axions in strongly magnetized neutron stars. The authors also quote a stronger limit, $g_{ae} < 9 \times 10^{-13}$ which is strongly dependent on the strength of the magnetic field in white dwarfs.

¹⁸⁸KEIL 97 uses new measurements of the axial-vector coupling strength of nucleons, as well as a reanalysis of many-body effects and pion-emission processes in the core of the neutron star, to update limits on the invisible-axion mass.

¹⁸⁹RAFFELT 95 reexamined the constraints on axion emission from red giants due to the axion-electron coupling. They improve on DEARBORN 86 by taking into proper account degeneracy effects in the bremsstrahlung rate. The limit comes from requiring the red giant core mass at helium ignition not to exceed its standard value by more than 5% (0.25 solar masses).

¹⁹⁰ALTHERR 94 bound is on the axion-electron coupling $g_{ae} < 1.5 \times 10^{-13}$, from energy loss via axion emission.

¹⁹¹CHANG 93 updates ENGEL 90 bound with the Kaplan-Manohar ambiguity in $z=m_{ij}/m_d$ (see the Note on the Quark Masses in the Quark Particle Listings). It leaves the window $f_A=3 \times 10^5-3 \times 10^6$ GeV open. The constraint from Big-Bang Nucleosynthesis is satisfied in this window as well.

¹⁹²BERSHADY 91 searched for a line at wave length from 3100-8300 Å expected from 2- γ decays of relic thermal axions in intergalactic light of three rich clusters of galaxies.

¹⁹³KIM 91c argues that the bound from the mass density of the universe will change drastically for the supersymmetric models due to the entropy production of saxion (scalar component in the axionic chiral multiplet) decay. Note that it is an upperbound rather than a lowerbound.

¹⁹⁴RAFFELT 91B argue that previous SN 1987A bounds must be relaxed due to corrections to nucleon bremsstrahlung processes.

¹⁹⁵RESSELL 91 uses absence of any intracluster line emission to set limit.

¹⁹⁶ENGEL 90 rule out $10^{-10} \lesssim g_{AN} \lesssim 10^{-3}$, which for a hadronic axion with EMC motivated axion-nucleon couplings corresponds to 2.5×10^{-3} eV $\lesssim m_{A0} \lesssim 2.5 \times 10^4$ eV. The constraint is loose in the middle of the range, i.e. for $g_{AN} \sim 10^{-6}$.

¹⁹⁷RAFFELT 90D is a re-analysis of DEARBORN 86.

Invisible A^0 (Axion) MASS LIMITS from Astrophysics and Cosmology

$v_1 = v_2$ is usually assumed ($v_j =$ vacuum expectation values). For a review of these limits, see RAFFELT 91 and TURNER 90. In the comment lines below, D and K refer to DFSZ and KSVZ axion types, discussed in the above minireview.

VALUE (eV)	CL%	DOCUMENT ID	TECN	COMMENT
<191	90	178 ANDRIAMON..09	CAST	K, solar axions
<334	95	179 DERBIN 09A	CNTR	K, solar axions
< 1.02	95	180 KEKEZ 09	HPGE	K, solar axions
< 1.2	95	181 HANNESTAD 08	COSM	K, hot dark matter
< 0.42	95	182 HANNESTAD 07	COSM	K, hot dark matter
< 1.05	95	183 MELCHIORRI 07A	COSM	K, hot dark matter
3 to 20		184 HANNESTAD 05A	COSM	K, hot dark matter
< 0.007		185 MORIO 98	COSM	K, hot dark matter
< 4		186 BORISOV 97	ASTR	D, neutron star
<(0.5-6) $\times 10^{-3}$		187 KACHELRIESS 97	ASTR	D, neutron star cooling
< 0.018		188 KEIL 97	ASTR	SN 1987A
< 0.010		189 RAFFELT 95	ASTR	D, red giant
		190 ALTHERR 94	ASTR	D, red giants, white dwarfs
< 0.01		191 CHANG 93	ASTR	K, SN 1987A
< 0.03		WANG 92	ASTR	D, white dwarf
		WANG 92c	ASTR	D, C-O burning

••• We do not use the following data for averages, fits, limits, etc. •••

¹⁹¹CHANG 93 updates ENGEL 90 bound with the Kaplan-Manohar ambiguity in $z=m_{ij}/m_d$ (see the Note on the Quark Masses in the Quark Particle Listings). It leaves the window $f_A=3 \times 10^5-3 \times 10^6$ GeV open. The constraint from Big-Bang Nucleosynthesis is satisfied in this window as well.

¹⁹²BERSHADY 91 searched for a line at wave length from 3100-8300 Å expected from 2- γ decays of relic thermal axions in intergalactic light of three rich clusters of galaxies.

¹⁹³KIM 91c argues that the bound from the mass density of the universe will change drastically for the supersymmetric models due to the entropy production of saxion (scalar component in the axionic chiral multiplet) decay. Note that it is an upperbound rather than a lowerbound.

¹⁹⁴RAFFELT 91B argue that previous SN 1987A bounds must be relaxed due to corrections to nucleon bremsstrahlung processes.

¹⁹⁵RESSELL 91 uses absence of any intracluster line emission to set limit.

¹⁹⁶ENGEL 90 rule out $10^{-10} \lesssim g_{AN} \lesssim 10^{-3}$, which for a hadronic axion with EMC motivated axion-nucleon couplings corresponds to 2.5×10^{-3} eV $\lesssim m_{A0} \lesssim 2.5 \times 10^4$ eV. The constraint is loose in the middle of the range, i.e. for $g_{AN} \sim 10^{-6}$.

¹⁹⁷RAFFELT 90D is a re-analysis of DEARBORN 86.

Gauge & Higgs Boson Particle Listings

Axions (A^0) and Other Very Light Bosons

- ¹⁹⁸ The region $m_{A^0} \gtrsim 2$ eV is also allowed.
- ¹⁹⁹ ERICSON 89 considered various nuclear corrections to axion emission in a supernova core, and found a reduction of the previous limit (MAYLE 88) by a large factor.
- ²⁰⁰ MAYLE 89 limit based on naive quark model couplings of axion to nucleons. Limit based on couplings motivated by EMC measurements is 2–4 times weaker. The limit from axion-electron coupling is weak: see HATSUDA 88B.
- ²⁰¹ RAFFELT 88B derives a limit for the energy generation rate by exotic processes in helium-burning stars $\epsilon < 100$ erg $g^{-1} s^{-1}$, which gives a firmer basis for the axion limits based on red giant cooling.
- ²⁰² RAFFELT 87 also gives a limit $g_{A\gamma} < 1 \times 10^{-10}$ GeV^{-1} .
- ²⁰³ DEARBORN 86 also gives a limit $g_{A\gamma} < 1.4 \times 10^{-11}$ GeV^{-1} .
- ²⁰⁴ RAFFELT 86 gives a limit $g_{A\gamma} < 1.1 \times 10^{-10}$ GeV^{-1} from red giants and $< 2.4 \times 10^{-9}$ GeV^{-1} from the sun.
- ²⁰⁵ KAPLAN 85 says $m_{A^0} < 23$ eV is allowed for a special choice of model parameters.
- ²⁰⁶ FUKUGITA 82 gives a limit $g_{A\gamma} < 2.3 \times 10^{-10}$ GeV^{-1} .

Search for Relic Invisible Axions

Limits are for $[G_{A\gamma\gamma}/m_{A^0}^2] \rho_A$ where $G_{A\gamma\gamma}$ denotes the axion two-photon coupling,

$L_{int} = \frac{G_{A\gamma\gamma}}{4} \phi_A F_{\mu\nu} \tilde{F}^{\mu\nu} = G_{A\gamma\gamma} \phi_A \mathbf{E} \cdot \mathbf{B}$, and ρ_A is the axion energy density near the earth.

VALUE	CL%	DOCUMENT ID	TECN	COMMENT
• • • We do not use the following data for averages, fits, limits, etc. • • •				
$< 1.9 \times 10^{-43}$	97.7	207 DUFFY	06 CNTR	$m_{A^0} = 1.98\text{--}2.17 \times 10^{-6}$ eV
$< 5.5 \times 10^{-43}$	90	208 ASZTALOS	04 CNTR	$m_{A^0} = 1.9\text{--}3.3 \times 10^{-6}$ eV
		209 KIM	98 THEO	
$< 2 \times 10^{-41}$		210 HAGMANN	90 CNTR	$m_{A^0} = (5.4\text{--}5.9) 10^{-6}$ eV
$< 1.3 \times 10^{-42}$	95	211 WUENSCH	89 CNTR	$m_{A^0} = (4.5\text{--}10.2) 10^{-6}$ eV
$< 2 \times 10^{-41}$	95	211 WUENSCH	89 CNTR	$m_{A^0} = (11.3\text{--}16.3) 10^{-6}$ eV
²⁰⁷ DUFFY 06 used the upgraded detector of ASZTALOS 04, while assuming a smaller velocity dispersion than the isothermal model as in Eq. (8) of their paper. See Fig. 10 of their paper on the axion mass dependence of the limit.				
²⁰⁸ ASZTALOS 04 looked for a conversion of halo axions to microwave photons in magnetic field. At 90% CL, the KSVZ axion cannot have a local halo density more than 0.45 GeV/cm^3 in the quoted mass range. See Fig. 7 of their paper on the axion mass dependence of the limit.				
²⁰⁹ KIM 98 calculated the axion-to-photon couplings for various axion models and compared them to the HAGMANN 90 bounds. This analysis demonstrates a strong model dependence of $G_{A\gamma\gamma}$ and hence the bound from relic axion search.				
²¹⁰ HAGMANN 90 experiment is based on the proposal of SIKIVIE 83.				
²¹¹ WUENSCH 89 looks for condensed axions near the earth that could be converted to photons in the presence of an intense electromagnetic field via the Primakoff effect, following the proposal of SIKIVIE 83. The theoretical prediction with $[G_{A\gamma\gamma}/m_{A^0}^2]^2 = 2 \times 10^{-14}$ MeV^{-4} (the three generation DFSZ model) and $\rho_A = 300$ MeV/cm^3 that makes up galactic halos gives $(G_{A\gamma\gamma}/m_{A^0}^2) \rho_A = 4 \times 10^{-44}$. Note that our definition of $G_{A\gamma\gamma}$ is $(1/4\pi)$ smaller than that of WUENSCH 89.				

Invisible A^0 (Axion) Limits from Photon Coupling

Limits are for the axion-two-photon coupling $G_{A\gamma\gamma}$ defined by $L = G_{A\gamma\gamma} \phi_A \mathbf{E} \cdot \mathbf{B}$.

For scalars S^0 the limit is on the coupling constant in $L = G_{S\gamma\gamma} \phi_S (\mathbf{E}^2 - \mathbf{B}^2)$.

VALUE (GeV^{-1})	CL%	DOCUMENT ID	TECN	COMMENT
• • • We do not use the following data for averages, fits, limits, etc. • • •				
$< 2.4 \times 10^{-9}$	95	212 AHMED	09A CDMS	$m_{A^0} < 100$ eV
$< 1.2\text{--}2.8 \times 10^{-10}$	95	213 ARIK	09 CAST	$m_{A^0} = 0.02\text{--}0.39$ eV
		214 CHOU	09	Chameleons
$< 7 \times 10^{-10}$		215 GONDOLO	09 ASTR	$m_{A^0} < \text{few keV}$
$< 1.3 \times 10^{-6}$	95	216 AFANASEV	08	$m_{S^0} < 1$ MeV
$< 3.5 \times 10^{-7}$	99.7	217 CHOU	08	$m_{A^0} < 0.5$ MeV
$< 1.1 \times 10^{-6}$	99.7	218 FOUICHE	08	$m_{A^0} < 1$ MeV
$< 5.6\text{--}13.4 \times 10^{-10}$	95	219 INOUE	08	$m_{A^0} = 0.84\text{--}1.00$ eV
$< 5 \times 10^{-7}$		220 ZAVATTINI	08	$m_{A^0} < 1$ MeV
$< 8.8 \times 10^{-11}$	95	221 ANDRIAMONJ	07 CAST	$m_{A^0} < 0.02$ eV
$< 1.25 \times 10^{-6}$	95	222 ROBILLIARD	07	$m_{A^0} < 1$ MeV
$2\text{--}5 \times 10^{-6}$		223 ZAVATTINI	06	$m_{A^0} = 1\text{--}1.5$ MeV
$< 1.1 \times 10^{-9}$	95	224 INOUE	02	$m_{A^0} = 0.05\text{--}0.27$ eV
$< 2.78 \times 10^{-9}$	95	225 MORALES	02B	$m_{A^0} < 1$ keV
$< 1.7 \times 10^{-9}$	90	226 BERNABEI	01B	$m_{A^0} < 100$ eV
$< 1.5 \times 10^{-4}$	90	227 ASTIER	00B NOMD	$m_{A^0} < 40$ eV
		228 MASSO	00 THEO	induced γ coupling
$< 2.7 \times 10^{-9}$	95	229 AVIGNONE	98 SLAX	$m_{A^0} < 1$ keV
$< 6.0 \times 10^{-10}$	95	230 MORIYAMA	98	$m_{A^0} < 0.03$ eV
$< 3.6 \times 10^{-7}$	95	231 CAMERON	93	$m_{A^0} < 10^{-3}$ eV, optical rotation
$< 6.7 \times 10^{-7}$	95	232 CAMERON	93	$m_{A^0} < 10^{-3}$ eV, photon regeneration
$< 3.6 \times 10^{-9}$	99.7	233 LAZARUS	92	$m_{A^0} < 0.03$ eV
$< 7.7 \times 10^{-9}$	99.7	233 LAZARUS	92	$m_{A^0} = 0.03\text{--}0.11$ eV
$< 7.7 \times 10^{-7}$	99	234 RUOSO	92	$m_{A^0} < 10^{-3}$ eV
$< 2.5 \times 10^{-6}$		235 SEMERTZIDIS	90	$m_{A^0} < 7 \times 10^{-4}$ eV

- ²¹² AHMED 09A is analogous to AVIGNONE 98.
- ²¹³ ARIK 09 is the 4He filling version of the CAST axion helioscope in analogy to INOUE 02 and INOUE 08. See their Fig. 7 for mass-dependent limits.
- ²¹⁴ CHOU 09 use the GammeV apparatus in the afterglow mode to search for chameleons, (pseudo)scalar bosons with a mass depending on the environment. For pseudoscalars they exclude at 3σ the range $2.6 \times 10^{-7} GeV^{-1} < G_{A\gamma\gamma} < 4.2 \times 10^{-6} GeV^{-1}$ for vacuum m_{A^0} roughly below 6 meV for density scaling index exceeding 0.8.
- ²¹⁵ GONDOLO 09 use the all-flavor measured solar neutrino flux to constrain solar interior temperature and thus energy losses.
- ²¹⁶ LIPSS photon regeneration experiment, assuming scalar particle S^0 . See Fig. 4 for mass-dependent limits.
- ²¹⁷ CHOU 08 perform a variable-baseline photon regeneration experiment. See their Fig. 3 for mass-dependent limits. Excludes the PVLAS result of ZAVATTINI 06.
- ²¹⁸ FOUICHE 08 is an update of ROBILLIARD 07. See their Fig. 12 for mass-dependent limits.
- ²¹⁹ INOUE 08 is an extension of INOUE 02 to larger axion masses, using the Tokyo axion helioscope. See their Fig. 4 for mass-dependent limits.
- ²²⁰ ZAVATTINI 08 is an upgrade of ZAVATTINI 06, see their Fig. 8 for mass-dependent limits. They now exclude the parameter range where ZAVATTINI 06 had seen a positive signature.
- ²²¹ ANDRIAMONJE 07 looked for Primakoff conversion of solar axions in 9T superconducting magnet into X-rays. Supersedes ZIOUTAS 05.
- ²²² ROBILLIARD 07 perform a photon regeneration experiment with a pulsed laser and pulsed magnetic field. See their Fig. 4 for mass-dependent limits. Excludes the PVLAS result of ZAVATTINI 06 with a CL exceeding 99.9%.
- ²²³ ZAVATTINI 06 propagate a laser beam in a magnetic field and observe dichroism and birefringence effects that could be attributed to an axion-like particle. This result is now excluded by ROBILLIARD 07, ZAVATTINI 08, and CHOU 08.
- ²²⁴ INOUE 02 looked for Primakoff conversion of solar axions in 4T superconducting magnet into X-ray.
- ²²⁵ MORALES 02B looked for the coherent conversion of solar axions to photons via the Primakoff effect in Germanium detector.
- ²²⁶ BERNABEI 01B looked for Primakoff coherent conversion of solar axions into photons via Bragg scattering in NaI crystal in DAMA dark matter detector.
- ²²⁷ ASTIER 00B looked for production of axions from the interaction of high-energy photons with the horn magnetic field and their subsequent re-conversion to photons via the interaction with the NOMAD dipole magnetic field.
- ²²⁸ MASSO 00 studied limits on axion-photon coupling using the induced axion-photon coupling through the proton loop and CAMERON 93 bound on the axion-photon coupling using optical rotation. They obtained the bound $g_P^2/4\pi < 1.7 \times 10^{-9}$ for the coupling $g_P \mathcal{P}^5 \rho \phi_A$.
- ²²⁹ AVIGNONE 98 result is based on the coherent conversion of solar axions to photons via the Primakoff effect in a single crystal germanium detector.
- ²³⁰ Based on the conversion of solar axions to X-rays in a strong laboratory magnetic field.
- ²³¹ Experiment based on proposal by MAIANI 86.
- ²³² Experiment based on proposal by VANBIBBER 87.
- ²³³ LAZARUS 92 experiment is based on proposal found in VANBIBBER 89.
- ²³⁴ RUOSO 92 experiment is based on the proposal by VANBIBBER 87.
- ²³⁵ SEMERTZIDIS 90 experiment is based on the proposal of MAIANI 86. The limit is obtained by taking the noise amplitude as the upper limit. Limits extend to $m_{A^0} = 4 \times 10^{-3}$ where $G_{A\gamma\gamma} < 1 \times 10^{-4} GeV^{-1}$.

Limit on Invisible A^0 (Axion) Electron Coupling

The limit is for $G_{Aee} \partial_\mu \phi_A \tilde{\epsilon}^{\mu\nu\lambda\sigma} e_\nu e_\lambda e_\sigma$ in GeV^{-1} , or equivalently, the dipole-dipole

potential $\frac{G_{Aee}^2}{4\pi} ((\boldsymbol{\sigma}_1 \cdot \boldsymbol{\sigma}_2) - 3(\boldsymbol{\sigma}_1 \cdot \mathbf{n})(\boldsymbol{\sigma}_2 \cdot \mathbf{n}))/r^3$ where $\mathbf{n} = \mathbf{r}/r$.

VALUE (GeV^{-1})	CL%	DOCUMENT ID	TECN	COMMENT
• • • We do not use the following data for averages, fits, limits, etc. • • •				
$< 1.4 \times 10^{-9}$	90	236 AHMED	09A CDMS	$m_{A^0} = 2.5$ keV
$< 3 \times 10^{-6}$		237 DAVOUDIALL	09 ASTR	Earth cooling
$< 0.6\text{--}2 \times 10^{-8}$	90	238 AALSETH	08 CNTR	$m_{A^0} = 0.3\text{--}7$ keV
$< 5.3 \times 10^{-5}$	66	239 NI	94	Induced magnetism
$< 6.7 \times 10^{-5}$	66	239 CHUI	93	Induced magnetism
$< 3.6 \times 10^{-4}$	66	240 PAN	92	Torsion pendulum
$< 2.7 \times 10^{-5}$	95	239 BOBRAKOV	91	Induced magnetism
$< 1.9 \times 10^{-3}$	66	241 WINELAND	91	NMR
$< 8.9 \times 10^{-4}$	66	240 RITTER	90	Torsion pendulum
$< 6.6 \times 10^{-5}$	95	239 VOROBYOV	88	Induced magnetism
²³⁶ AHMED 09A is analogous to AALSETH 08, using the CDMS detector. See their Fig. 5 for mass-dependent limits.				
²³⁷ DAVOUDIALL 09 use geophysical constraints on Earth cooling by axion emission.				
²³⁸ AALSETH 08 assume keV-mass pseudoscalars are the local dark matter and constrain the axio-electric effect in the CoGeNT detector. See their Fig. 3 for mass-dependent limits.				
²³⁹ These experiments measured induced magnetization of a bulk material by the spin-dependent potential generated from other bulk material with aligned electron spins, where the magnetic field is shielded with superconductor.				
²⁴⁰ These experiments used a torsion pendulum to measure the potential between two bulk matter objects where the spins are polarized but without a net magnetic field in either of them.				
²⁴¹ WINELAND 91 looked for an effect of bulk matter with aligned electron spins on atomic hyperfine splitting using nuclear magnetic resonance.				

See key on page 405

Gauge & Higgs Boson Particle Listings Axions (A⁰) and Other Very Light Bosons

Invisible A⁰ (Axion) Limits from Nucleon Coupling

Limits are for the axion mass in eV.

VALUE (eV)	CL%	DOCUMENT ID	TECN	COMMENT
● ● ● We do not use the following data for averages, fits, limits, etc. ● ● ●				
<159	95	242 DERBIN	09 CNTR	Solar axion
< 1.39 × 10 ⁴	90	243 BELLI	08A CNTR	Solar axion
		244 BELLINI	08 CNTR	Solar axion
		245 ADELBERGER	07	Test of Newton's law
<360	90	246 DERBIN	07 CNTR	Solar axion
<216	95	247 NAMBA	07 CNTR	Solar axion
< 1.6 × 10 ⁴	90	248 DERBIN	05 CNTR	Solar axion
<400	95	249 LJUBICIC	04 CNTR	Solar axion
< 3.2 × 10 ⁴	95	250 KRCMAR	01 CNTR	Solar axion
<745	95	251 KRCMAR	98 CNTR	Solar axion

242 DERBIN 09 is analogous to KRCMAR 98.

243 BELLINI 08A is analogous to KRCMAR 01 and DERBIN 05.

244 BELLINI 08 consider solar axions emitted in the M1 transition of ⁷Li* (478 keV) and look for a peak at 478 keV in the energy spectra of the Counting Test Facility (CTF), a Borexino prototype. For m_A⁰ < 450 keV they find mass-dependent limits on products of axion couplings to photons, electrons, and nucleons.

245 ADELBERGER 07 use precision tests of Newton's law to constrain a force contribution from the exchange of two pseudoscalars. See their Fig. 5 for limits on the pseudoscalar coupling to nucleons, relevant for m_A⁰ below about 1 meV.

246 DERBIN 07 is analogous to KRCMAR 98.

247 NAMBA 07 is analogous to KRCMAR 98.

248 DERBIN 05 bound is based on the same principle as KRCMAR 01.

249 LJUBICIC 04 looked for ejection of K-shell electrons by the axioelectric effect of 14.4 keV solar axions in a Germanium detector. The limit assumes the hadronic axion model and the same solar axion flux as in KRCMAR 98 and KRCMAR 01.

250 KRCMAR 01 looked for solar axions emitted by the M1 transition of ⁷Li after the electron capture by ⁷Be and the emission of 384 keV line neutrino, using their resonant capture on ⁷Li in the laboratory. The mass bound assumes m_u/m_d = 0.56 and the flavor-singlet axial-vector matrix element S = 0.4.

251 KRCMAR 98 looked for solar axions emitted by the M1 transition of thermally excited ⁵⁷Fe nuclei in the Sun, using their possible resonant capture on ⁵⁷Fe in the laboratory, following MORIYAMA 95b. The mass bound assumes m_u/m_d = 0.56 and the flavor-singlet axial-vector matrix element S = 3F - D ≈ 0.5.

Axion Limits from T-violating Medium-Range Forces

The limit is for the coupling $g = g_p g_s$ in a T-violating potential between nucleons or nucleon and electron of the form $V = \frac{g\hbar^2}{8\pi m_\rho} (\boldsymbol{\sigma} \cdot \hat{\mathbf{r}}) (\frac{1}{r_2} + \frac{1}{r_1}) e^{-r/\lambda}$, where g_p and g_s are dimensionless scalar and pseudoscalar coupling constants and $\lambda = \hbar/(m_A c)$ is the range of the force.

VALUE	DOCUMENT ID	TECN	COMMENT
● ● ● We do not use the following data for averages, fits, limits, etc. ● ● ●			
	252 SEREBROV 10		ultracold neutrons
	253 IGNATOVICH 09	RVUE	ultracold neutrons
	254 SEREBROV 09	RVUE	ultracold neutrons
	255 BAESSLER 07		ultracold neutrons
	256 HECKEL 06		torsion pendulum
	257 NI 99		paramagnetic Tb F ₃
	258 POSPELOV 98	THEO	neutron EDM
	259 YOUDIN 96		torsion pendulum
	260 RITTER 93		torsion pendulum
	261 VENEMA 92		nuclear spin-precession frequencies
	262 WINELAND 91	NMR	

252 SEREBROV 10 use spin precession of ultracold neutrons close to bulk matter and find $g < 2 \times 10^{-21} (\text{cm}/\lambda)^2$ at 95% CL for the force range $\lambda = 10^{-4} - 1$ cm.

253 IGNATOVICH 09 use data on depolarization of ultracold neutrons in material traps. They show λ -dependent limits in their Fig. 1.

254 SEREBROV 09 use data on depolarization of ultracold neutrons stored in material traps and finds $g < 2.96 \times 10^{-21} (\text{cm}/\lambda)^2$ for the force range $\lambda = 10^{-3} - 1$ cm and $g < 3.9 \times 10^{-22} (\text{cm}/\lambda)^2$ for $\lambda = 10^{-4} - 10^{-3}$ cm, each time at 95% CL, significantly improving on BAESSLER 07.

255 BAESSLER 07 use the observation of quantum states of ultracold neutrons in the Earth's gravitational field to constrain g for an interaction range 1 μm - a few mm. See their Fig. 3 for results.

256 HECKEL 06 studied the influence of unpolarized bulk matter, including the laboratory's surroundings or the Sun, on a torsion pendulum containing about 9×10^{22} polarized electrons. See their Fig. 4 for limits on g as a function of interaction range.

257 NI 99 searched for a T-violating medium-range force acting on paramagnetic Tb F₃ salt. See their Fig. 1 for the result.

258 POSPELOV 98 studied the possible contribution of T-violating Medium-Range Force to the neutron electric dipole moment, which is possible when axion interactions violate CP. The size of the force among nucleons must be smaller than gravity by a factor of $2 \times 10^{-10} (1 \text{ cm}/\lambda_A)$, where $\lambda_A = \hbar/m_A c$.

259 YOUDIN 96 compared the precession frequencies of atomic ¹⁹⁹Hg and Cs when a large mass is positioned near the cells, relative to an applied magnetic field. See Fig. 3 for their limits.

260 RITTER 93 studied the influence of bulk mass with polarized electrons on an unpolarized torsion pendulum, providing limits in the interaction range from 1 to 100 cm.

261 VENEMA 92 looked for an effect of Earth's gravity on nuclear spin-precession frequencies of ¹⁹⁹Hg and ²⁰¹Hg atoms.

262 WINELAND 91 looked for an effect of bulk matter with aligned electron spins on atomic hyperfine resonances in stored ⁹Be⁺ ions using nuclear magnetic resonance.

REFERENCES FOR Searches for Axions (A⁰) and Other Very Light Bosons

SEREBROV	10	JETPL 91 6	A. Serebrov <i>et al.</i>	(CDMS Collab.)
AHMED	09A	PRL 103 141802	Z. Ahmed <i>et al.</i>	
ANDRIAMON	09	JCAP 0912 002	S. Andriamonje <i>et al.</i>	
ARGYRADES	09	PR 080 032501R	J. Argyrades <i>et al.</i>	(NEMO-3 Collab.)
ARIK	09	JCAP 0902 008	E. Arik <i>et al.</i>	(CAST Collab.)
AUBERT	09Z	PRL 103 081803	B. Aubert <i>et al.</i>	(BABAR Collab.)
CHOU	09	PRL 102 030402	A.S. Chou <i>et al.</i>	(GammeV Collab.)
DAVOUDIASH	09	PR D79 095024	H. Davoudiasl, P. Huber	
DERBIN	09	EPJ C62 755	A.V. Derbin <i>et al.</i>	
DERBIN	09A	PL B678 181	A.V. Derbin <i>et al.</i>	
GONDOLO	09	PR D79 107301	P. Gondolo, G. Raffelt	(UTAH, MPIM)
IGNATOVICH	09	EPJ C64 19	V.K. Ignatovich, Y.N. Pokotilovskii	(JINR)
KEKEZ	09	PL B671 345	D. Kekez <i>et al.</i>	
SEREBROV	09	PL B680 423	A. Serebrov	(PNPI)
TUNG	09	PRL 102 051802	Y.C. Tung <i>et al.</i>	(KEK E391a Collab.)
AALSETH	08	PRL 101 251301	C.E. Aalseth <i>et al.</i>	(CoGeNT Collab.)
AFANASEV	08	PRL 101 120401	A. Afanasev <i>et al.</i>	
BELLI	08A	NP A806 388	P. Belli <i>et al.</i>	
BELLINI	08	EPJ C54 61	G. Bellini <i>et al.</i>	(Borexino Collab.)
CHOU	08	PRL 100 080402	A.S. Chou <i>et al.</i>	(GammeV Collab.)
FOUCHE	08	PR D78 032013	M. Fouche <i>et al.</i>	
HANNENSTAD	08	JCAP 0804 019	S. Hannestad <i>et al.</i>	
INOUE	08	PL B668 93	Y. Inoue <i>et al.</i>	
LOVE	08	PRL 101 151801	M. Love <i>et al.</i>	(CLEO Collab.)
ZAVATTINI	08	PR D77 032006	E. Zavattini <i>et al.</i>	(PVLAS Collab.)
ADELBERGER	07	PRL 98 131104	E.G. Adelberger <i>et al.</i>	
ANDRIAMON	07	JCAP 0704 010	S. Andriamonje <i>et al.</i>	(CAST Collab.)
BAESSLER	07	PR D75 075006	S. Baessler <i>et al.</i>	
CHANG	07	PR D75 052004	H.M. Chang <i>et al.</i>	(TEXONO Collab.)
DERBIN	07	JETPL 85 12	A.V. Derbin <i>et al.</i>	
HANNENSTAD	07	JCAP 0708 015	S. Hannestad <i>et al.</i>	
JAIN	07	JPG 34 129	P.L. Jain, G. Singh	
LESSA	07	PR D75 094001	A.P. Lessa, O.L.G. Peres	
MELCHIORRI	07A	PR D76 041303R	A. Melchiorri, O. Menz, A. Slosar	
NAMBA	07	PL B645 398	T. Namba	
ROBILLIARD	07	PRL 99 190403	C. Robilliard <i>et al.</i>	
ARNOLD	06	NP A765 483	R. Arnold <i>et al.</i>	(NEMO-3 Collab.)
DUFFY	06	PR D74 012006	L.D. Duffy <i>et al.</i>	
HECKEL	06	PRL 97 021603	B.R. Heckel <i>et al.</i>	
ZAVATTINI	06	PRL 96 110406	E. Zavattini <i>et al.</i>	(PVLAS Collab.)
DERBIN	05	JETPL 81 365	A.V. Derbin <i>et al.</i>	
Translated from ZETFP 81 453.				
HANNENSTAD	05A	JCAP 0507 002	S. Hannestad, A. Mirizzi, G. Raffelt	
PARK	05	PRL 94 021801	H.K. Park <i>et al.</i>	(FNAL HyperCP Collab.)
ZIOUTAS	05	PRL 94 121301	K. Zioutas <i>et al.</i>	(CAST Collab.)
ADLER	04	PR D70 037102	S. Adler <i>et al.</i>	(BNL E787 Collab.)
ANISIMOVSK...	04	PRL 93 031801	V.V. Anisimovskiy <i>et al.</i>	(BNL E949 Collab.)
ARNOLD	04	JETPL 80 377	R. Arnold <i>et al.</i>	(NEMO3 Detector Collab.)
Translated from ZETFP 80 429.				
ASZTALOS	04	PR D69 011101R	S.J. Asztalos <i>et al.</i>	
LJUBICIC	04	PL B599 143	A. Ljubicic <i>et al.</i>	
ARNABOLDI	03	PL B557 167	C. Arnaboldi <i>et al.</i>	
CIVITARESE	03	NP A729 987	O. Civitarese, J. Suhonen	
DANEVICH	03	PR C68 035501	F.A. Danevich <i>et al.</i>	
ADLER	02C	PL B537 211	S. Adler <i>et al.</i>	(BNL E787 Collab.)
BADERT...	02	PL B542 29	A. Badertscher <i>et al.</i>	
BERNABEI	02D	PL B546 23	R. Bernabei <i>et al.</i>	(DAMA Collab.)
DERBIN	02	PAN 65 1302	A.V. Derbin <i>et al.</i>	
Translated from YAF 65 1335.				
FUSHIMI	02	PL B531 190	K. Fushimi <i>et al.</i>	(ELEGANT V Collab.)
INOUE	02	PL B536 18	Y. Inoue <i>et al.</i>	
MORALES	02B	ASP 16 325	A. Morales <i>et al.</i>	(COSME Collab.)
ADLER	01	PR D63 032004	S. Adler <i>et al.</i>	(BNL E787 Collab.)
AMMAR	01B	PRL 87 271801	R. Ammar <i>et al.</i>	(CLEO Collab.)
ASHITKOV	01	JETPL 74 529	V.D. Ashitkov <i>et al.</i>	
Translated from ZETFP 74 601.				
BERNABEI	01B	PL B515 6	R. Bernabei <i>et al.</i>	(DAMA Collab.)
DANEVICH	01	NP A694 375	F.A. Danevich <i>et al.</i>	
DEBOER	01	JPG 27 L29	F.W.N. de Boer <i>et al.</i>	
KRCMAR	01	PR D64 115016	M. Krcmar <i>et al.</i>	
STOICA	01	NP A694 269	S. Stoica, H.V. Klapprod-Kleingrothaus	
ALESSAND...	00	PL B466 13	A. Alessandrello <i>et al.</i>	
ARNOLD	00	NP A678 341	R. Arnold <i>et al.</i>	
ASTIER	00B	PL B479 371	P. Astier <i>et al.</i>	(NOMAD Collab.)
DANEVICH	00	PR C62 045501	F.A. Danevich <i>et al.</i>	
MASSO	00	PR D61 011701R	E. Masso	
ARNOLD	99	NP A658 299	R. Arnold <i>et al.</i>	(NEMO Collab.)
NI	99	PRL 82 2439	W.-T. Ni <i>et al.</i>	
SIMKOVIC	99	PR C60 055502	F. Simkovic <i>et al.</i>	
ALTEGOER	98	PL B428 197	J. Altegoer <i>et al.</i>	
ARNOLD	98	NP A636 209	R. Arnold <i>et al.</i>	(NEMO-2 Collab.)
AVIGNONE	98	PRL 81 5068	F.T. Avignone <i>et al.</i>	(Solar Axion Experiment)
DIAZ	98	NP B527 44	M.A. Diaz <i>et al.</i>	
FAESSLER	98B	JPG 24 2139	A. Faessler, F. Simkovic	
KIM	98	PR D58 055006	J.E. Kim	
KRCMAR	98	PL B442 38	M. Krcmar <i>et al.</i>	
LUESCHER	98	PL B434 407	R. Luescher <i>et al.</i>	
MORIYAMA	98	PL B434 147	S. Moriyama <i>et al.</i>	
MOROJ	98	PL B440 69	T. Moroi, H. Murayama	
POSPLOV	98	PR D58 097703	M. Pospelov	
ZUBER	98	PRPL 305 295	K. Zuber	(APEX Collab.)
AHMAD	97	PRL 78 618	I. Ahmad <i>et al.</i>	(MOSU)
BORISOV	97	JETP 83 868	A.V. Borisov, V.Y. Grishinia	
DEBOER	97C	JPG 23 135	F.W.N. de Boer <i>et al.</i>	
KACHELRIESS	97	PR D56 1313	H. Kachelriess, C. Wille, G. Wunner	(BOCH)
KEIL	97	PR D56 2419	W. Keil <i>et al.</i>	
KITCHING	97	PRL 79 4079	P. Kitching <i>et al.</i>	(BNL E787 Collab.)
LEINBERGER	97	PL B394 16	U. Leibneger <i>et al.</i>	(ORANG Collab.)
ADLER	96	PRL 76 1421	S. Adler <i>et al.</i>	(BNL E787 Collab.)
AMSLER	96B	ZPHY C70 219	C. AMSLER <i>et al.</i>	(Crystal Barrel Collab.)
GANZ	96	PL B389 4	R. Ganz <i>et al.</i>	(GS1, HEID, FRAN, JAGL+)
GUENTHER	96	PR D54 3641	M. Gunther <i>et al.</i>	(MPIH, SASSO)
KAMEL	96	PL B368 291	S. Kamel	(SHAMS)
MITSUI	96	EPL 33 111	T. Mitsui <i>et al.</i>	(TOKY)
YOUDIN	95	PRL 77 2170	A.M. Youdin <i>et al.</i>	(AMHT, WASH)
ALTMANN	95	ZPHY C68 221	M. Altmann <i>et al.</i>	(MUNT, LAPP, CPPM)
BALEST	95	PR D51 2053	R. Balest <i>et al.</i>	(CLEO Collab.)
BASSOMPIE...	95	PL B355 584	G. Bassompierre <i>et al.</i>	(LAPP, LGCT, LYON)
MAENO	95	PL B351 574	T. Maeno <i>et al.</i>	(TOKY)
MORIYAMA	95B	PRL 75 3222	S. Moriyama	
RAFFELT	95	PR D51 1495	G. Raffelt, A. Weiss	(MPIM, MPIA)
SKALSEY	95	PR D51 6292	M. Skalsey, R.S. Conti	(MICH)
TSUNODA	95	EPL 30 273	T. Tsunoda <i>et al.</i>	(TOKY)
ADACHI	94	PR A49 3201	S. Adachi <i>et al.</i>	(TMU)
ALTHERR	94	ASP 2 175	T. Altherr, E. Petitgirard, T. del Rio	(Gaztelurrutia)
AMSLER	94B	PL B333 271	C. AMSLER <i>et al.</i>	(Crystal Barrel Collab.)
ASAI	94	PL B323 90	S. Asai <i>et al.</i>	(TOKY)
MEUDERDRES	94	PR D49 4937	M.R. Dreses <i>et al.</i>	(BRCO, OREG, TRIU)
NO	94	Physica B194 153	W.T. Ni <i>et al.</i>	(NTHU)
VO	94	PR C49 1551	D.T. Vo <i>et al.</i>	(ISU, LBL, LLNL, UCD)

